J. agric. Engng Res. (2001) **79** (3), 239–263
doi:10.1006/jaer.2001.0722, available online at http://www.idealibrary.com on IDEAL®
SW—Soil and Water

REVIEW PAPER

Soil Adhesion and Biomimetics of Soil-engaging Components: a Review

Lu-Quan Ren; Jin Tong; Jian-Qiao Li; Bing-Cong Chen

Research Institute for Agricultural Machinery Engineering, Jilin University (Nanling Campus), Changchun 130025, Peoples Republic of China; e-mail of corresponding author: jtong@jlu.edu.cn

(Received 30 August 1999; accepted in revised form 15 March 2001; published online 6 June 2001)

Adhesive forces exist between soil and the surfaces of soil-engaging components on a variety of terrain machines including tillage and sowing machines. This phenomenon of soil adhesion not only increases the working resistance and energy consumption of these machines, but also decreases the quality of work. Characteristics of soil adhesion to solid surfaces, behaviour and principles of soil-burrowing animals for improved soil scouring and biomimetics of soil-engaging components are reviewed in this paper. The characteristics of soil adhesion to solid surfaces were concerned with: the morphological features of soil at the contact interfaces, contact models of soil adhesion, explanation of soil adhesion, factors affecting soil adhesion and conventional methods for reducing adhesion. Details on the behaviour of soil-burrowing animals include: claw shape; body surface geometry, chemical constitution, liquid secretion and bioelectricity; and body flexing behaviour. The principles of soil-burrowing animals in soil scouring mainly comprise the effects of geometrical morphologies and shapes, hydrophobicity, micro-electro-osmotic systems, lubrication and body surface flexibility. Based on these characteristics, biomimetic methods for reducing soil adhesion to soil-engaging components include: biomimetic non-smooth surfaces; modification of soil-engaging materials; biomimetic non-smooth electro-osmosis; and flexible components.

1. Introduction

The phenomenon of soil adhesion exists when soil is in contact with a solid interface. At the interface, the sliding resistance is dependent on the adhesion, the stress normal to the interface and the angle of friction between the soil and the interface. By reducing the adhesion and interface friction angle to values less than the soil cohesion and soil to soil friction angle, respectively, the sliding resistance of soil engaging implements is reduced (Hendrick & Bailey, 1982). For tillage equipment, the quality of work is decreased and the energy consumption is increased due to soil adhesion. Adhesion of soil to components of sowing machines, such as the furrow opener and covering device, decreases the emergence rate of seeds considerably. The quality of fertilizing and transplanting is also decreased due to soil adhesion. Techniques for reducing soil adhesion are also important in the harvesting of root crops, such as sugar beet (Vermeulen *et al.*, 1997). The output of soil-engaging components of earthmoving machines, such as excavator buckets, bulldozer blades, and self-unloading boxes of dump trucks, may be decreased by 30–50% due to soil adhesion, and sometimes they cannot work at all. Soil adhesion increases the rolling resistance of vehicles on soft ground, for example, in paddy fields, swamps and sea beaches. Excessive adhesion of soil to the running gear can immobilize the vehicle completely.

Soil adhesion properties—including the adhesion mechanism, contributory factors and methods for reducing soil adhesion—have been investigated by many researchers. Gill and Vanden Berg (1967) and Chancellor (1994) also reviewed the research on soil adhesion and interfacial friction.

The problem of soil adhesion has been solved by the soil-burrowing animals. They have a significant ability to prevent soil from sticking to their bodies because of the evolution of their biological systems through the exchange of matter, energy and information with soil over millions of years. They can move in soil without soil sticking to their bodies, especially in clay. Observation of the anti-adhesive characteristics of soil-burrowing

Notation

a	constant	r_a	ratio of areas
b	constant	t	time, s
D	fractal dimension	V	volume content of reinforcement in a composite material
F	tensile force, N		
h_1	distance between two solid surfaces, m	α	tilt angle, deg
h_2	distance between two solid surfaces, m	β	constant
J	some property of the interlayer water	γ_{LV}	surface tension of water, $N\,m^{-1}$
J_0	property J of bulk water	η	viscosity of liquid, Pa s
L	length of segment, m	θ_A	contact angle of advancing water, deg
$M(r<R)$	cumulative mass of soil particles, kg	θ_R	contact angle of receding water, deg
M_T	mass of the total soil particles, kg	θ_0	inherent contact angle of water on surface, deg
m_m	mass of soil, kg		
m_w	mass of water, kg	θ_1	contact angle of water on matrix material, deg
N_L	number of embossed convex domes		
P	capillary pressure, Pa	θ_2	contact angle of water on reinforcing material, deg
R	characteristic size of particle, m		
R_d	disc radius, m	θ_a	apparent contact angle of water on rough surface, deg
R_L	the size of the largest soil particle, m		
R_T	radius of the theoretical capillary tube, m	θ_c	contact angle of water on composite surface, deg
r	soil particle size, m		

animals led to the study of the principles involved and the potential application of techniques to soil-engaging components. The geometric, physico-chemical and mechanical features of soil-burrowing animals were utilized to design soil-engaging materials and structures. This generated the biomimetics of soil-engaging components for reduced adhesion or 'anti-adhesion' and interfacial friction. This paper reviews soil adhesion, the principles of soil-burrowing animals and biomimetics of soil-engaging components in anti-adhesion of soil, and further challenges to biomimetics in this field were analysed.

2. Adhesion of soil to solid surfaces

2.1. *Morphological features of soil at the contact interfaces and contact models*

2.1.1. *Surface morphologies of soil at the contact interfaces*

The soil surface morphologies formed at the contact interface with solid surfaces were examined by scanning electron microscopy (Tong *et al*., 1990a, 1994c). It was found that the soil surface cut with a fine steel wire displayed a rougher structure [*Fig. 1*(*a*)]. When a Teflon disc was pressed onto the cut soil surface under a certain normal stress, the plastic flow of the topsoil took place and the dimensions of pores of the surface layer became smaller. The topsoil was changed from a loose pattern of particle packing to a compact pattern of particle packing, from an unsaturated state to a saturated state, and from discontinuous water menisci to a continuous water film. *Figures 1*(*b*) and (*c*) illustrate two typical surface morphologies. The roughness of the soil surfaces formed at the contact interface existed in three sizes: the microaggregate; the particle; and the asperity on the particles. The surface feature was dependent upon their topography and arrangement. Actually, the roughness of soil surfaces can extend to the molecular scale. The surface of soil particles is a molecular fractal surface with a self-similar fractal structure (Pfeifer, 1984; Avnir *et al*., 1985). The fractal dimension of between two and three, was a quantitative parameter of the fractal surfaces.

The surface morphologies of soil taken off a rubber surface after air drying were also examined (Tong *et al*., 1993). It was found that many closed structural units were formed at the contact interface [*Fig. 1*(*d*)].

2.1.2. *Contact models of soil with solid surfaces*

On the basis of the water film states and the surface morphology at the contact interface, there were two contact situations at the interface (Tong *et al*., 1994c). When the moisture content of soil or the normal stress applied to the interface was low, a continuous water film

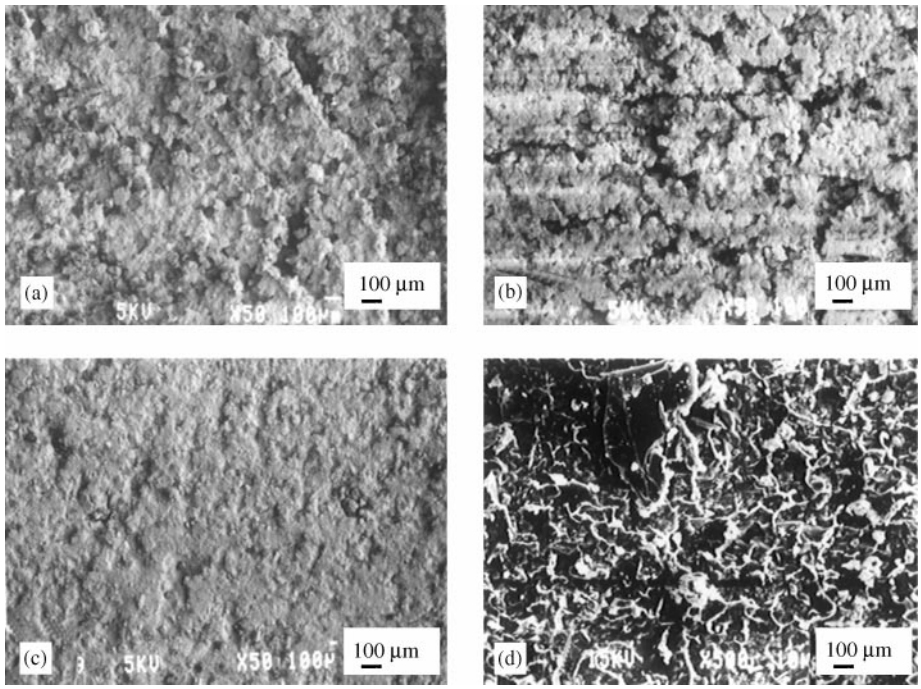

Fig. 1. Photographs by scanning electron microscopy of the morphologies of soil surfaces formed after (a) cutting with a steel wire, (b, c) contacting with a disc of Teflon, and (d) contacting with a rubber surface, using (a, b, c) yellow clay soil with a moisture content of 27·1% d. b. and (d) supersaturated black soil (Tong et al., 1993, 1994c)

was not formed at the interface and there exist five possible contact states: completely non-contacting asperities; water point contacting asperities; water menisci contacting asperities; water menisci contacting particles; and local water film contacting micro-aggregates. When the moisture content of the soil or the normal stress was high, the contact interface was filled with water and the soil was linked with the solid surface by a continuous water film.

2.2. *Explanations of soil adhesion*

2.2.1. *Moisture tension of the interfacial water film*

Fountaine (1954) demonstrated that water film plays a dominant role in soil adhesion. When a continuous water film is formed between a saturated soil and a solid surface and reaches equilibrium, the moisture tension would come to the same value through the soil mass including the contact interface. In this condition, the shapes of all the water–air menisci satisfy the equation:

$$P = 2\gamma_{LV}/R_T \tag{1}$$

where γ_{LV} is the surface tension of water, R_T is the radius of the theoretical capillary tube and P is the capillary pressure. The soil adhesion as a force per unit area caused by the water film is equal to the moisture tension. From Eqn (1), the adhesion is very strong when the water film is very thin and vice versa.

2.2.2. *Molecular attraction and negative air pressure*

There exists molecular attraction between the solid surface and non-contacting asperities or water point contacting asperities of soil, but the molecular attraction would be strong only if the separation between them reaches the equilibrium intermolecular distance. The molecular attraction can contribute markedly to the soil adhesion. If their separation is very much larger than the equilibrium intermolecular distance, the molecular attraction force would be negligible for the soil adhesion. There may exist a very large force of molecular attraction between a rubber surface and the wall of the closed structural units in the soil surface layer shown in *Fig. 1*(*d*) because the separation reaches the equilibrium intermolecular distance. In addition, the negative air pressure existing within the closed structural units may also play an important role. In this condition, the molecular attraction and the negative air pressure are the main reasons for adhesion of soil to rubber.

2.2.3. *Capillary attraction from the interfacial water film*

Akiyama and Yokoi (1972a, 1972b) represented soil particles in the geometrically simplified form of spheres

with the same size. They analysed the soil adhesion for the continuous water film and water menisci contact states, respectively, for the ideal soil with the close packing and with the loose packing situations. They considered that the water film capillary pressure was the source of the soil adhesion for the continuous film contact state; and that the capillary pressure and the surface tension were the sources of soil adhesion for the water menisci contact state. Actually, both the moisture tension and the capillary pressure are due to the surface tension of the continuous water film or water menisci and, therefore, the conclusions by Fountaine (1954) and by Akiyama and Yokoi (1972a, 1972b) were similar. Both indicated the important action of the water surface tension on soil adhesion.

2.2.4. *Viscous resistance of the interfacial water film*

It was verified that when the gap between two solid surfaces was immersed completely in a liquid, no surface tension existed in the interfacial liquid film in the gap. The normal tensile force required to separate the two solid surfaces was dependent upon the speed at which they were separated (Bowden & Tabor, 1954). For two discs of radius R_d immersed in a liquid of viscosity η, the time t required to increase the separation from a distance h_1 to h_2 between two solid surfaces under the tensile force of F is given by Eqn (2), as long as the liquid film does not break during pulling:

$$t = \left(\frac{3\pi\eta R_d^2}{4F}\right)\left(\frac{1}{h_1^2} - \frac{1}{h_2^2}\right) \tag{2}$$

If the two solid surfaces are separated in a short time, a very large force would be required. This indicates that the viscous resistance of the liquid contributes to the adhesion. From Eqn (2), it can be also found that the tensile force F is directly proportional to the liquid viscosity for a given time t. The adhesion will be increased with the liquid viscosity.

2.2.5. *Nature and properties of water as a function of the thickness of water film*

Low (1979) studied the nature and properties of water in montmorillonite–water systems. It was found that, when the water film was very thin, the molecular structure of water in the film varied due to the inducing effect of the montmorillonite molecules and the distortion and fracture of the hydrogen bonds between the induced molecules became more difficult. The thermodynamic, dynamic and spectral properties—including partial specific heat, partial specific volume and, especially, viscosity of the water—followed the trend described by the general equation:

$$J = J_0 \exp\left(\frac{\beta}{m_w/m_m}\right) \tag{3}$$

where J is some property of the interlayer water, J_0 is the same property of the bulk water, β is a constant depending upon the nature of the solid surfaces and m_w/m_m is the ratio of the mass of water to the mass of soil. The ratio m_w/m_m represented the thickness of the interlayer water film. Equation (3) shows that the properties of the water film are increased as the thickness of the water film is decreased.

2.3. *Factors affecting soil adhesion*

On the basis of the above explanation of soil adhesion, it was understood that the adhesion between soil and solid surfaces was dependent upon the nature and properties of soil, the material properties of the soil-engaging components and the experimental conditions or working surroundings. The factors affecting soil adhesion were included in these three aspects.

2.3.1. *Effects of soil properties*

Soil factors affecting the soil adhesion included the soil texture, moisture content and water tension, porosity, organic matter content and others (Chancellor, 1994). It was found that there was different soil adhesion for different minerals. The soil adhesion was increased as the proportion of clay particles in the soil was increased and was highest when the soil moisture content was between the plastic limit and the liquid limit. An increase in the soil water tension elevated the soil adhesion.

As a working tool to investigate irregular morphologies and structures, fractal geometry (Mandelbrot, 1982) has been applied extensively to the research of soil science. The soil physical properties (bulk density, pore-size distribution, aggregate-size distribution, ped shape and soil micro-topography) can be described by fractals; soil processes (adsorption, diffusion, transport of water and solutes, brittle fracture and fragmentation) can be modelled by fractals; and the soil spatial variability can be quantified by fractals (Perfect & Kay, 1995). As an indicator of soil texture, the soil particle-size distribution displays fractal structure in many cases. Tyler and Wheatcraft (1992) derived a relationship between the cumulative mass of soil particles and the particle size as follows:

$$\frac{M(r < R)}{M_T} = \left(\frac{R}{R_L}\right)^{3-D} \tag{4}$$

where $M(r < R)$ is the cumulative mass of soil particles of size r equal to or more than a characteristic size R, M_T is the mass of the total soil particles, R_L is the size of the largest particle and D is the fractal dimension of the soil particle-size distribution. If the particle-size distribution

Table 1
Advancing contact angles θ_A and receding contact angles θ_R of water on the surfaces of some solid materials

Solid material	*Advancing contact angle (θ_A), deg*	*Receding contact angle (θ_R), deg*	*Reference*
Polytetrafluoroethylene (Teflon)	109	106	Wu (1982)
Polystyrene	91	84	Wu (1982)
Polyethylene	96	62	Wu (1982)
Polypropylene	108		Adamson (1976)
Paraffin wax	110		Adamson (1976)
Polycarbonate	84	68	Wu (1982)
Human skin	90		Adamson (1976)
Gold	66		Adamson (1976)
Platinum	40		Adamson (1976)
Plain carbon steel	73	0	Tong *et al.* (1994c)
Enamel	29	0	Tong *et al.* (1994c)

of a soil is a fractal, then the log–log plot of $M(r < R)$ and R/R_L is a straight line. The fractal dimension D can be calculated from the slope of the straight line. Generally, the fractal dimensions of particle size distributions of soils are increased with the clay particle content and, therefore, the soil adhesion and frictional force are increased (Tong *et al.*, 1994a, 1999; Yan *et al.*, 1996). The molecular fractal dimension of soil particle surfaces is also an important factor affecting soil adhesion. The larger the molecular fractal dimension, the larger is the specific surface area, and the higher the soil adhesion as well.

2.3.2. *Effects of properties of soil-engaging component surfaces*

The atomic or molecular structure of surfaces of a solid or a liquid is different to that of their bulk materials because the structural symmetry of atoms or molecules is lost and, therefore, physical and chemical properties of surfaces are changed. This has resulted in such surface phenomena as physical adsorption, chemical adsorption, chemical reaction and soil adhesion as well. On the basis of the surface free energy, surfaces may be classified into high-energy surfaces and low-energy surfaces, corresponding to high surface energy materials and low surface energy materials. High surface energy materials include metals, metallic compounds and inorganic compounds (*i.e.* oxides, nitrides, silica and diamond) and their surface tension is from 0·2 to 0·5 $\mathrm{N\,m^{-1}}$. Low surface energy materials include organic compounds and organic polymers, and their surface tension is, mostly, less than 0·1 $\mathrm{N\,m^{-1}}$. Water is a low surface energy material and has a surface tension of 0·0728 $\mathrm{N\,m^{-1}}$ at 20°C. High-energy surfaces are hydrophilic and low-energy surfaces are hydrophobic. The hydrophilicity or hydrophobicity of a surface can be expressed by the contact angle of water on the surface. The higher the contact angle of water on the surface, the higher is the hydrophobicity of the surface, that is, the lower the hydrophilicity of the surface. Table 1 lists advancing contact angles θ_A and receding contact angles θ_R of water on the surfaces of some solid materials. Mostly, the adhesion between soil and hydrophobic materials is poor, that is to say, the larger the contact angles, the lower is the soil adhesion. Therefore, metallic materials, metallic compounds and inorganic compounds display higher soil adhesion, and polymeric materials have a lower soil adhesion.

Li *et al.* (1993a, 1993b, 1996b) tested the effects of microstructure on the adhesion of soil to steel-35. It was found that the soil adhesion to steel-35 with a tempered martensite microstructure and with a tempered sorbite microstructure was lower than that of the microstructure was obtained through quenching and low-temperature tempering treatment, the tempered troostite through the quenching and average temperature tempering treatment, and the tempered sorbite through the quenching and high-temperature tempering treatment. *Figure 2* illustrates the relationship between soil adhesion and the tempering temperature for steel-35. Soil adhesion to steel-35 is higher within the average tempering temperature range.

2.3.3. *Effects of experimental conditions and working surroundings*

Factors affecting soil adhesion include such experimental conditions and working surroundings as the applied normal stress, the application time for that stress, temperature, electric field, magnetic field and vibration. Sliding resistance is a monotonically increasing function of normal stress for most solid materials (Zhang *et al.*, 1986). Sometimes, the soil adhesion was increased to a certain value and then decreased as the normal pressure was increased (Li *et al.*, 1993b), possibly for the reason of the interfacial lubrication by water squeezed out of the

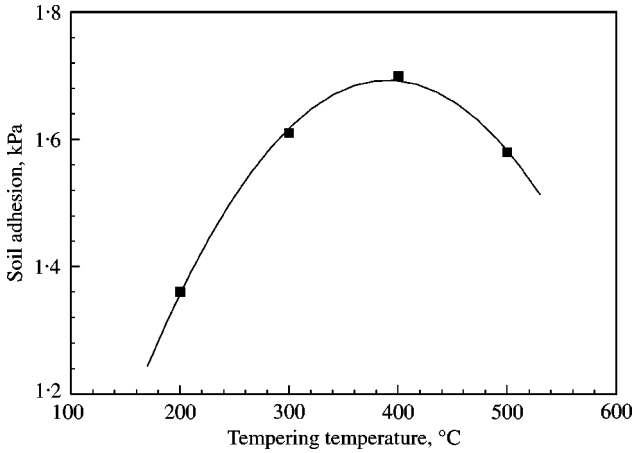

Fig. 2. Soil adhesion of steel-35 after tempering at various temperatures (Li et al., 1996b)

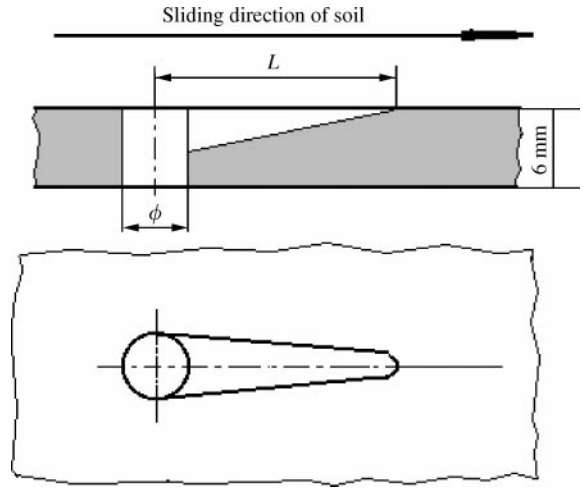

Fig. 3. Schematic diagram of 'comet-type' oblique hole drilled through a plough mouldboard (Zhu et al., 1992)

soil. The surface tension of water is a function of temperature. The surface tension of water is decreased as the temperature is elevated, and so is the viscosity of water. Therefore, an increase of temperature can make the surface tension of the interfacial water film decrease and, as a result, the soil adhesion can be reduced. When an electric field generated by a negative pole and positive pole is applied to soil, the soil water can move from the positive pole to the negative pole. This is called the electro-osmotic phenomenon of soil. If the non-scouring areas of soil contact are given negative polarity, the thickness of the water film increases owing to electro-osmosis, which can reduce the soil adhesion (Shen, 1982; Cong *et al*., 1990a). The nature and properties of the soil can be changed under a strong magnetic field, for example: the variable negative electric charge and the permeability are increased; and the positive electric charge and the expandability are decreased (Zhuang *et al*., 1992). These changes, in general, reduce the adhesion of soil to solid materials (Han & Zhang, 1991; Zhang & Han, 1992; Guo & Liu, 1995). Ultrasonic vibration and mechanical vibration can reduce the soil adhesion and interface friction or separate the adhered soil from the solid surfaces (Sharma *et al*., 1977; Wang *et al*., 1993, 1996).

2.4. *Conventional methods for reducing soil adhesion*

2.4.1. *Surface shape design*

Improvement of the surface design of soil-engaging components is one of the conventional methods for reducing soil adhesion and interface friction. This method is, mostly, based on the kinematic and dynamic analysis of the interactive relation between soil and soil-engaging components. Some convex corrugations made on the soil-contacting surfaces can decrease the real contact area and break the continuity of the interfacial water film between soil and solid surfaces, which results in a reduction of the soil adhesion and sliding resistance against solid surfaces (Cong *et al*., 1990b). Zhu *et al*. (1992) reported a plough with some 'comet-type' oblique holes drilled through the ploughshare and the breast of the mouldboard. *Figure 3* illustrates the schematic diagram of these holes. It was shown that the ploughing resistance was reduced by 2·5–3·5% and by 8–12% in a moist field soil and under paddy field conditions, respectively.

2.4.2. *Soil-engaging component materials*

Modification of soil engaging component materials is an important method for reducing soil adhesion and interface friction. Many researchers have examined the soil adhesion characteristics of polymeric materials, owing to their lower surface energy. The tested polymeric materials included Teflon (polytetrafluoroethylene—PTFE), ultra high molecular weight polyethylene (UHMWPE), polyethersulphone–polytetrafluoroethylene (PES–PTFE) coating and others (Fox & Bockhup, 1965; Salokhe & Gee-Clough, 1989; Tong *et al*., 1990b, 1994c; Lu *et al*., 1996; Liu *et al*., 1998b). The applications of polymeric materials for soil-engaging components were limited due to their poor abrasion resistance against soil (Tong *et al*., 1994b, 1999).

Salokhe and Gee-Clough (1988, 1989) and Salokhe *et al*. (1990, 1993) examined the soil adhesion characteristics of enamel coating. It was found that the enamel coating has the ability to reduce soil adhesion. Rolling resistance of cage wheels and the plough boat can be reduced owing to the enamel coating on the wheel lugs and on the boat surfaces and their tractive performance

was improved. However, the spalling rupture of the enamel coating easily took place under the abrasive wear conditions (Tong *et al*., 1998). The abrasion resistance of enamel coating may be increased by modifying the rare materials for the coating and by improving the preparation techniques.

Cast iron materials are most commonly used for simple soil tillage implements. It was found that white iron, one of the conventional plough mouldboard materials, containing more phosphorus and silicon, improved the anti-adhesive properties (Tong *et al*., 1990c; Chen *et al*., 1995a). However, it was noted that an excessive phosphorus content tended to increase the brittleness of white iron, limiting the application of phosphoric white iron to soil-engaging components.

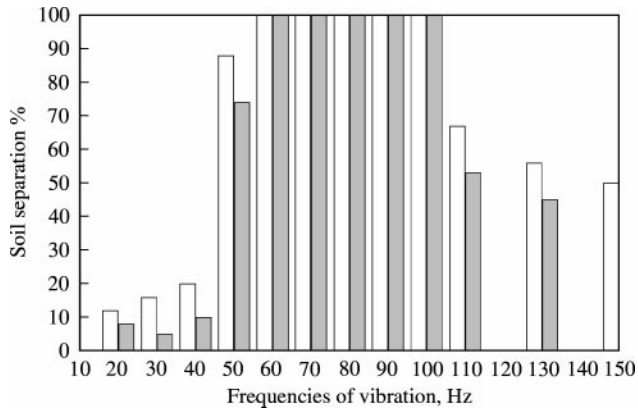

Fig. 4. Soil separation versus frequencies of vibration showing the effects of vibration on scouring of soil-engaging components (Wang et al., 1996); soil spraying speed during preconditioning: ■, *5·0–5·9 m s*$^{-1}$; □, *6·0–7·0 m s*$^{-1}$

2.4.3. *Electro-osmosis*

The electro-osmotic effect is influenced by: the soil moisture content; soil texture; electric voltage and contact time for electro-osmosis; the separation between the zones of positive and negative polarity and their area ratio; and the contact pressure as well. A high voltage for electro-osmosis and a long contact time are required in order to increase the thickness of the interfacial water film between the soil and the zone of negative polarity. The soil adhesion to the zone of negative polarity could be reduced by shortening the separation between the two terminals. The electro-osmotic effect is better for clay soil than for sandy soil (Cong *et al*., 1990a, 1990b). The application of the electro-osmotic method to a sliding component in contact with soil was limited because of the long contact time required for electro-osmosis. The method of electro-osmosis may be applied successfully only to reducing adhesion of soil to the soil-engaging components with a long contact time between them, for example, excavator buckets (Cong *et al*., 1990b). Much more energy is consumed when high voltage is used for electro-osmosis and further research is required into the effective use of lower voltages. It was reported that the voltage can be decreased by changing the position of the zones of polarity and their arrangement (Cong *et al*., 1990b). Clyma and Larson (1991) also reported that the voltage could be decreased to 45 V.

2.4.4. *Magnetic fields*

Han and Zhang (1991) and Guo and Liu (1995) tested the effect of a magnetic field on ploughing resistance. Several permanent magnets were attached to the back of the ploughshare. Han and Zhang (1991) reported that the ploughing resistance and the fuel consumption of the tractors used for pulling the ploughs were reduced by 10·55% and 11·30%, respectively, for the magnetized plough as compared to the non-magnetized plough under the identical field conditions (in a medium loam, with a moisture content of 15·98% d.b.). Guo and Liu (1995) reported that the fuel consumption of the tractors can be reduced by 7–15% for the magnetized plough in a field soil with a moisture content of 12·26–14·28% d.b. and for a ploughing depth of 25–30 mm.

Zhang and Han (1992) tested the effect of the magnetic field on the forward resistance of the covering blade in a medium loam soil at a moisture content of 12% d.b. The forward resistance of the magnetized covering blade can be reduced by 15·4–23·3% as compared with the conventional one with the same dimensions. It was also found that the largest reduction in the forward resistance occurred at a magnetic induction of 23 mT.

2.4.5. *Vibration*

Sharma *et al*. (1977) tested the effect of ultrasonic vibration on the friction of metal against soil. The vibration frequency used was 10 kHz. Wang *et al*. (1993, 1996) designed a mechanism used for testing the effect of mechanical vibration on soil adhesion. The vibration was produced by blowing compressed air. The soil used for the tests was a silty loam with a moisture content of 38·7% d.b. Vibration at frequencies of between 60 and 100 Hz was remarkably effective in removing soil from the plate (*Fig. 4*).

2.4.6. *Lubrication*

Araya and Kawanishi (1984) and Schafer *et al*. (1977) studied the effect of the flow of air, water and polymer–water solution on the friction between soil and solid surfaces. The fluids injected between soil and soil-engaging components had a lubricating action and, therefore, could cause the draught reduction of soil-engaging equipment. Air or water lubrication was used to reduce the soil adhesion to excavator buckets (Cong *et al*., 1990b). The disadvantage of the flow lubrication method

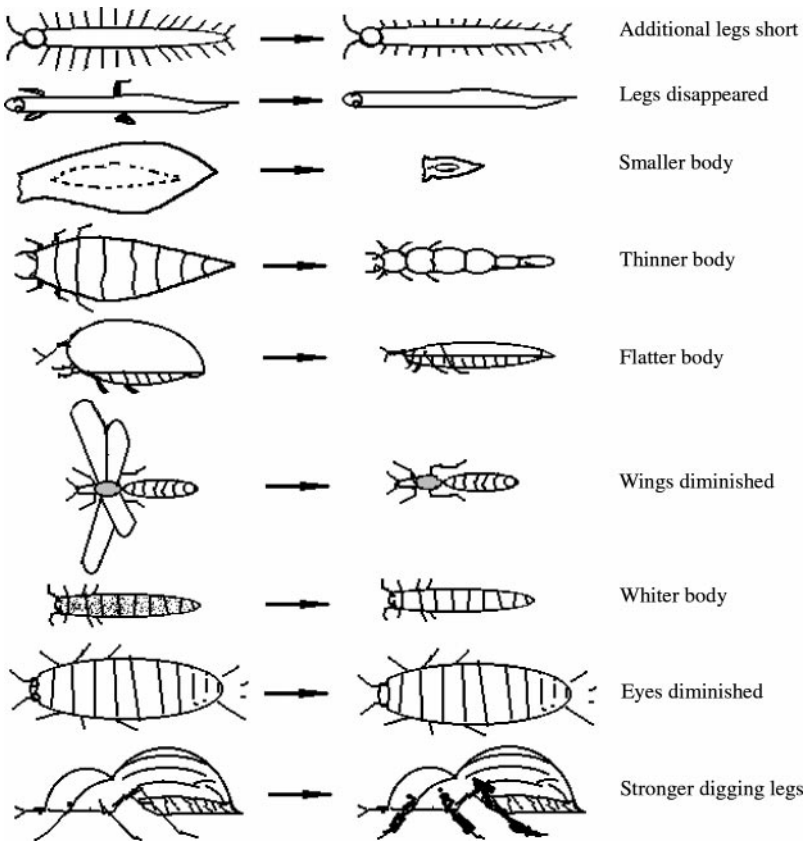

Fig. 5. Some special macroscopic features of soil animals in evolution (Xin, 1986)

was the additional equipment required to reduce soil adhesion and interfacial friction.

2.4.7. *Additional mechanisms*

An additional mechanism can be attached to remove the soil adhering to the soil-engaging components (Cong *et al*., 1990b). This method was applied mostly to excavator buckets and blades. Ren *et al*. (1990d) designed a bucket with a flexible floor and demonstrated that it could reduce soil accretion in the bucket by 59·4% and loading resistance by 15·85%. Yin *et al*. (1990) designed a tongue scraper mechanism for a loader bucket to remove the soil accretion in the bucket. The shovel with this mechanism was tested in handling soil and powdered coal and was found to increase loader productivity by 20%.

3. Characteristics of soil-burrowing animals

3.1. *Evolution of soil-burrowing animals*

Soil-burrowing animals include those soil animals living mainly in the soil and other animals, such as the nocturnal pangolin, digging a large subterranean chamber or cave in the earth as a den. The living surroundings of soil animals are different to those of animals on land and in water. Soil is a semi-solid material in which it is dark, moist and difficult for animal movement. However, soil animals have ability to adapt to the soil surroundings because of their evolution in biological systems over millions of years. Two different adaptations for soil have occurred in soil animals, the active adaptation and the passive adaptation. Some features of soil animals in evolution are shown in *Fig. 5*. The stronger digging legs were as a result of active adaptation for burrowing, for example, the forelegs of mole crickets (*Gryllotalpidae*) and the claws of black ground beetles (*Carabidae*), dung beetles (*Scarabaeidae*) and *Cydnidae* (Xin, 1986). The passive adaptation of animals to the soil habitat resulted in shorter or vestigial additional legs, the body becoming smaller, thinner or flatter, and wings and eyes diminishing.

As there is continuous interaction between the soil animals and the soil in which they move, subsistence would be decreased and existence threatened if soil could not be removed from body surfaces. The anti-adhesive characteristics of their body surfaces are an inevitable outcome of their evolution over millions of years.

3.2. *Geometry of body surfaces*

3.2.1. *Basic concepts of surface uniformity*

Ren *et al.* (1992b) described the basic concepts of surface texture with respect to soil adhesion, defining smooth and non-smooth surfaces. A surface texture meeting the living requirements of animals or the working conditions of soil-engaging components is called smooth when there exists no surface irregularities which adversely influence the tangential resistance to movement. If there exist some construction units, such as convex domes and dimpled concavities arranged on a smooth surface, the surface can be considered as a geometrically non-smooth surface. Geometrically non-smooth construction units, distributed either regularly or randomly to form a continuous geometrical surface, mechanically affect soil movement and change sliding resistance compared with that for a smooth surface.

Surface irregularities can occur not only by varying the surface texture but also by using materials of different chemical composition and electrical conductivity and through dynamic effects. Composite materials can cause non-uniform wetting behaviour. Surface characteristics altering from smooth to non-smooth as the rate of shear increases are called dynamically non-smooth surfaces, as typified by the skin of a dolphin which has a smooth cuticle surface with many hard fibro-nodules underneath. When a dolphin is moving, the fibro-nodules become harder and bigger to produce a geometrically non-smooth surface.

3.2.2. *Morphologies of body surfaces*

All soil-burrowing animals have geometrically non-smooth structures or rough structures on their body surfaces. Chen *et al.* (1990b), Ren *et al.* (1990c, 1992a), Cong *et al.* (1992) and Tong *et al.* (1994d) observed and examined the geometrical surface morphologies of earthworm (*Lumbricidae*), *Oniscidae*, *Diplopoden*, centipede (*Chilopoda*), dung beetle (*Scarabaeidae*), ground beetle (*Carabidae*), ant (*Formicidae*), mole cricket (*Gryllotalpidae*), *Labidura riparia*, cockroach (*Blattaria*), cricket (*Gryllidae*), and pangolin. There exist differences between different species of soil-burrowing animals in the shape and the size of the non-smooth construction units. According to the shape of the unit, the geometrically non-smooth surfaces can be classified as embossed (with small convex domes), dimpled (with small concave hollows), wavy, scaly, corrugated (with ridges), stepped and seta-covered; according to the size, there are macroscopic and microscopic non-smooth surfaces; and according to the arrangement of the units, there are regular and random geometrically non-smooth surfaces. *Figure 6* shows some photographs of typical morphologies of body surfaces of soil-burrowing animals and pangolin scales. The non-smooth construction units may be rigid, elastic or flexible.

3.2.3. *Shapes of claws*

Ren *et al.* (1990b) observed and examined the shapes and surface morphologies of claws of the mole cricket, ant, dung beetle and pangolin. It was found that the fore part of the claws of these animals is wedge shaped. The fore parts of the claws of the ant and pangolin are tapered wedges with a wedge angle of 20°, those of the mole cricket are square wedges with a wedge angle of 30°, and those of the dung beetle are flat wedges with a wedge angle of 50°. The extent of the claw wedge angle of soil-burrowing animals has a certain relationship with the claw depth for dislodging soil particles and with the animal habitat, *i.e.* the properties of the soil. The curvature is largest at the claw tip and becomes smaller and smaller with the distance from the claw tip. There are ridges, furrows and some cilia on the surfaces of soil-burrowing animals' claws. *Figure 7* shows scanning electron microscopy photographs of claws of a mole cricket.

3.3. *Chemical composition of body surfaces*

It was determined by Xu *et al.* (1990), Tong *et al.* (1994d, 1995) and Cui *et al.* (1990) that the cuticle of the dung beetle, black ant, mole cricket, ground beetle and pangolin scales contains carbon, hydrogen, nitrogen, oxygen and some trace elements, such as potassium, chlorine, calcium, silicon, phosphorus, sulphur, sodium, magnesium, aluminium, manganese and iron. The relative contents of the trace elements vary from animal to animal and from one part to the other parts of the same animal. A living body contains, generally, 60–70% of water and some organic substances including organic compounds. Organic substances in the living body are mainly protein, nucleic acid, saccharine and lipoid. Organic compounds include amino acids, fatty acids, glucose, hormones, vitamins, glycerine, urea, uric acid, creatine and some other organic acids. The protein is a high molecular compound and mainly consists of carbon, hydrogen, oxygen and nitrogen, sometimes, a small amount of trace elements. The outermost surface layer of soil animals' cuticle consists of a material similar to resin or paint and possesses a strong hydrophobic property. The contact angles of water on the surfaces of soil animals' cuticle are more than 90°. Pangolin scales mainly consist of α-keratin and β-keratin, which contain 18 amino acids (Tong *et al.*, 1995) (Table 2). The effects of amino acids on the anti-adhesion of soil animals are not currently known.

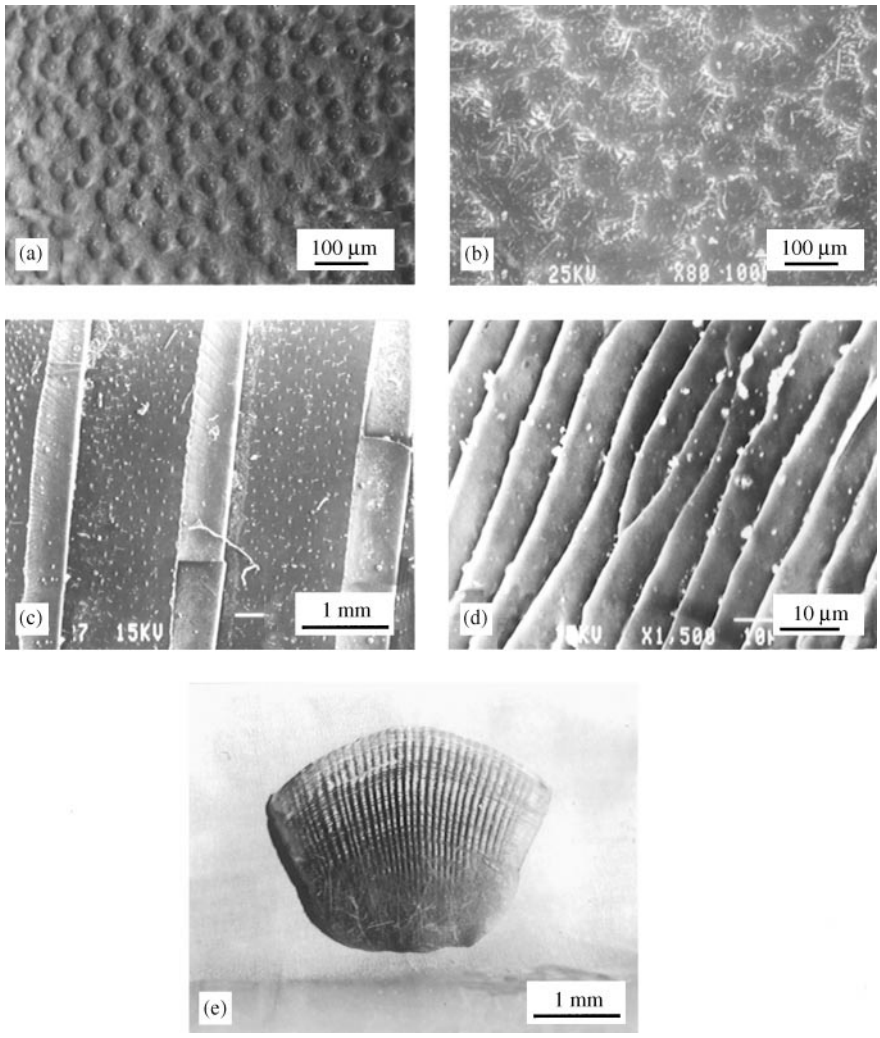

Fig. 6. Some characteristic non-smooth morphologies of body surfaces of soil-burrowing animals: (a) surface embossed with small convex domes on the head of a dung beetle; (b) surface dimpled with small concave hollows on the head of a dung beetle; (c) ridged surface on the abdomen of a ground beetle; (d) stepped surface on the head of a black ant: and (e) a pangolin scale (Tong et al., 1994d, 1995)

3.4. *Liquid substance on body surfaces*

3.4.1. *Methods for collecting secretion liquid of earthworm*

The earthworm is a typical animal covered with a liquid secretion on its body surface. In order to examine its chemical composition and anti-adhesive properties, Chen *et al.* (1990a) tested three methods for collecting the liquid secretion of earthworm (*Eisena foetida*), the electrical stimulation method, the transference method and the immersion method. For the electrical stimulation method, two electrodes were attached to the body and then the earthworm was stimulated with electricity so that the liquid substance was secreted. For the transference method, a layer of food in a glass jar was separated by a steel wire gauze from an upper layer of clean dry sand. Some earthworms were laid on the dry sand for 24 h and the liquid substance secreted by the earthworms was transferred onto the sand grains. The sand grains with the liquid secretion were placed into a diluted saline solution and, 24 h afterwards, sand grains and earthworm casts were filtered. The solution was desalinated and then concentrated to obtain the enriched secretion substance. For the immersion method, clean earthworms were immersed into a saline solution with a concentration of 0·2% (w/w) for 24 h. Thereafter, the earthworms were dredged up and their casts filtered from the solution. The solution containing the secretion substance was desalinated, then concentrated and the enriched secretion substance obtained as for the transference method. Chen *et al.* (1990a) demonstrated that any of these three

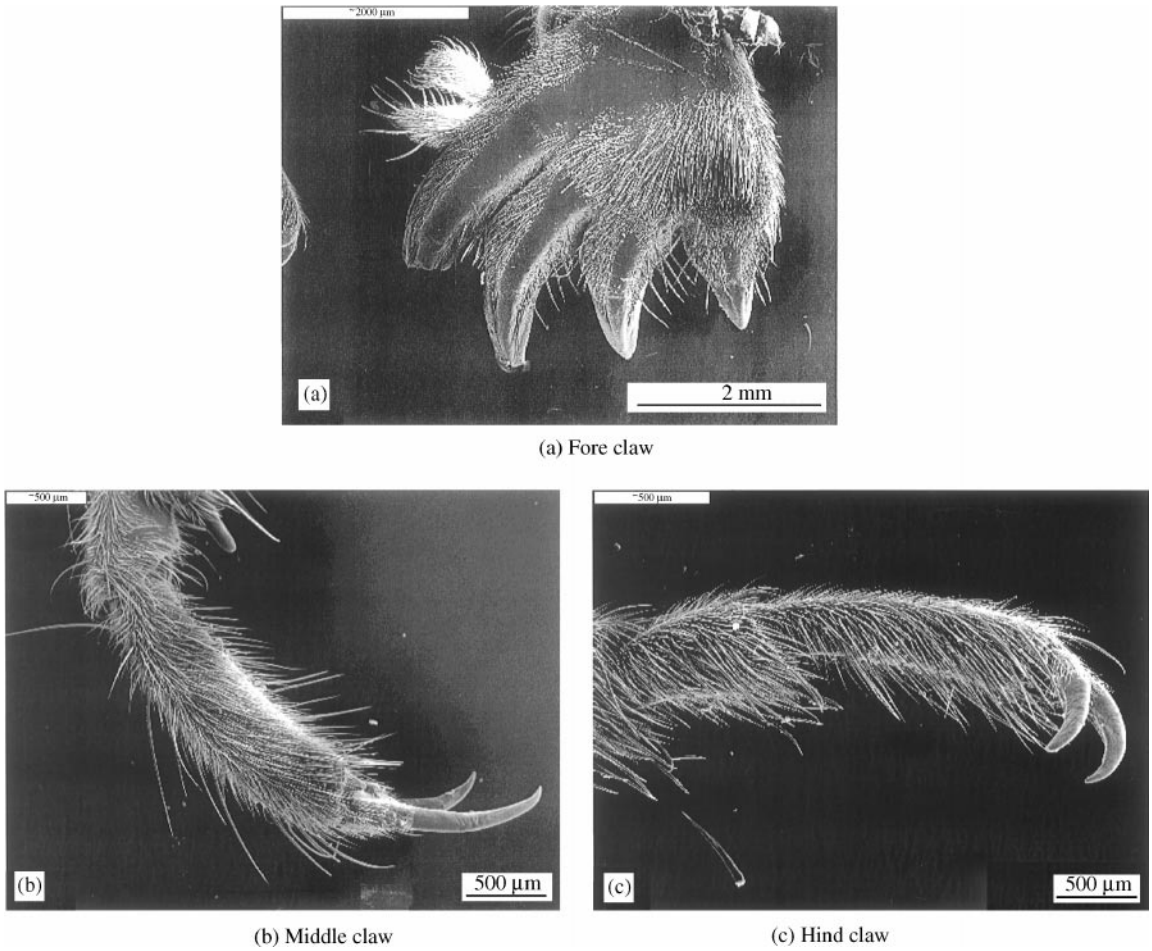

Fig. 7. Photographs showing shapes and topography of claws of a mole cricket: (a) fore claw, (b) middle claw, and (c) hind claw (Ren et al., 1990)

methods could be used for collecting the secretions of earthworms.

3.4.2. *Chemical composition of earthworm secretions*

Li *et al.* (1990) examined the chemical composition of the liquid secretion of the earthworm (*Eisena foetida*). The secretion consisted of water (99·71% by weight) and a little of an organic substance with a molecular weight of 30 000–50 000. Some 59% of the organic substance was protein containing 18 amino acids and the rest was the conjugated saccharide and a little of other water-soluble substances. The protein was combined with the conjugated saccharide to yield a conjugated protein, which was a mucoprotein. The water-soluble substances were mainly the metabolite, such as ammonia, urea and uric acid coming from the body of the earthworm and organic salt from the soil. Table 3 gives the amino acid composition of the secretions, the whole body of the earthworm (*Eisena foetida*) and the secretions of the loach (*Misqurnus fossilis*).

3.5. *Bioelectricity of body surfaces*

3.5.1. *Bioelectrical phenomenon*

Various vital activities in nature are accompanied by electrical phenomena, that is to say, there exists bioelectricity in all living creatures. There are two basic voltages of bioelectricity, the resting potential and the action potential. The surface potential of a living body is a combined reflection of the resting potential and the action potential in the body. The resting potential is the potential difference between the outside and the inside of the tissue or cell membrane of a living creature when it is resting. The action potential is the potential difference between the excited part and the resting part of the same tissue or cells. The action potential is of short duration and reversible, and larger than the membrane potential. The resting potential and the action potential of muscle and nerve cells are 60–90 and 90–120 mV, respectively (Ma, 1984). Yamashiro (1989, 1995) reported the piezoelectric effect of a crab shell, lily and bamboo leaf.

Table 2
Amino acid composition of pangolin scale, hair and feather (Tong *et al.*, 1995)

	Keratin content, % by weight		
Amino acid	*Pangolin scale*	*Hair*	*Feather*
Glycine	10·6–13·7	5·2–6·5	7·2
Alanine	2·3–3·0	3·4–4·4	5·4
Valine	3·2–4·0	5·0–5·9	8·8
Leucine	7·8–7·9	7·6–8·1	8·0
Isoleucine	2·0–2·3	3·1–4·5	6·0
Serine	5·0–5·5	7·2–9·5	14·0
Threonine	3·2–3·4	6·6–6·7	4·8
Tyrosine	17·2–20·0	4·0–6·4	2·2
Phenylalanine	3·0–3·2	3·4–4·0	5·3
Cysteine	1·9	—	—
Cystine	—	11·4–14·1	8·2
Methionine	0·4–0·6	0·5–0·7	0·5
Tryptophan	0·4–0·5	1·8–2·1	0·7
Arginine	8·0–8·6	9·2–10·0	7·5
Histidine	0·7–1·2	2·8–3·3	0·7
Lysine	2·5–2·6	0·7–1·1	1·7
Aspartoyl	7·1–7·9	6·4–7·3	7·5
Glutamic acid	10·4–10·9	13·1–16·0	9·7
Proline	8·6–9·7	5·8–8·1	10·0

3.5.2. *Surface electric potential of earthworms*

Sun *et al.* (1991) measured the surface potential of the fore part, the middle part and the hind part of earthworms (*Michaelsen*) using non-polarized silver/silver chloride electrodes and silk electrodes. *Figure 8* shows a manner of fixing the electrodes to the skin of the earthworm. The measuring electrode was a half ring. It was found that the resting potential of the earthworm tended to zero with respect to the earth. When it was creeping, the skin of the earthworm possessed a negative potential at the moving body part with respect to the earth and the resting part. The maximum amplitude of the surface potential was 40 mV, occurring at its fore part. A circular non-polarized silver/silver chloride electrode was also prepared and fixed inside a 10 mm long tube. The inside diameter of this tube was a little less than the cross-sectional size of the earthworm tested. The earthworms were guided through the tube and the surface potential was recorded. In this case, the maximum amplitude of the surface potential was 35 mV at the fore part, 19 mV at the middle part and 18 mV at the hind part. Table 4 gives the average potential measured.

3.6. *Flexibility of soil-burrowing animals*

The flexible features of the skin of pangolin (*Manis pentadactyla linnacus*), vole (*Microtas manderinns*) and *Cylindroiulus teutonicus* and others were analysed by Ren *et al.* (1996, 1998). Pangolin is a typical soil-burrowing animal of 700–900 mm in body length and often digging subterranean chambers up to 10 m in length. In China, the pangolin lives in wet woodlands in an area of red soil which is very cohesive and sticky. The body of the pangolin is covered with a layer of scales, some with corrugations regularly arranged on the scale surface [*Fig. 6*(*e*)]. Pangolin scales also exhibit a flexible feature by turning upwards and whipping under the muscular action of the dermis beneath the layer of scales. A vole lives in wet areas, such as low-lying land, contour furrows and paddy-field borders. The skin of the vole is covered in hair, including needle hair and villi, which has been keratinized. The density of the vole hair is 80–100 per mm^2.

Many soil animals such as the centipede (*Chilopoda*), *Cylindroiusus teutonicus*, earthworm and the larvae of most insects adopt a creeping mode of movement, progressing forwards on expansion and contraction of their musculus longitudinalis and musculus transversus. The body of *Cylindroiusus teutonicus* is circular and has 25–100 segments. Two double paraeiopods protrude from the abdomen of the *Cylindroiusus teutonicus*, with strong intersegmental membranes and cuticle of hard chitin. On the skin of most soil animals, including the cricket, dung beetle and ground beetle, setae or cilia exist.

A scale, segment, seta or a cilium can be considered a construction unit of their body skin (Ren *et al.*, 1996). These units all possess a flexible motion. The geometrically non-smooth surface formed by flexible construction units was called the flexible non-smooth surface and the corresponding flexibility was called the non-smooth flexibility. In other words, the flexibility of the skin of soil animals is brought about through their geometrically non-smooth construction units.

4. Principles of anti-adhesive characteristics of soil animals

4.1. *Geometrical morphologies and shapes*

Ren *et al.* (1990a), Tong *et al.* (1994d) and Jia *et al.* (1995b, 1996a) analysed the effects of the microscopic geometrically non-smooth or rough structure of body surfaces of soil animals on their wetting behaviour. The contour of the non-smooth body surfaces of soil animals was assumed as a wavy profile. A model for the non-smooth body surfaces of soil animals (non-smooth or rough) is shown in *Fig. 9*. The apparent contact angle θ_a for the corrugated surface could be expressed as

$$\cos\theta_a = r_a \cos_0 \qquad (5)$$

Table 3
Amino acid composition of the secretion substances and the whole body of *Eisena foetida*, of the cuticle of *Lumbricus terrestis* and the secretion substances of the loach *Misquirnus fossilis*

	Composition, % by weight			
Amino acid	*Secretion from Eisena foetida*	*Whole body of Eisena foetida*	*Cuticle of Lumbricus terrestris*	*Secretion of Misgurnus fossilis*
Glycine	6·68	5·39	22·39	4·89
Alanine	5·85	6·55	8·82	8·27
Valine	5·85	3·82	2·46	6·70
Leucine	7·10	8·05	4·27	10·31
Isoleucine	5·22	4·95	2·22	6·29
Serine	5·43	4·61	10·63	5·04
Threonine	9·60	4·98	7·08	5·34
Tyrosine	3·34	4·08	0·72	—
Phenylalanine	3·55	4·43	2·19	5·37
Cysteine	1·04	—		—
Cystine	—	1·42		—
Meithonine	3·76	0·75		2·30
Tryptophan	1·25	1·11		0·69
Arginine	3·97	8·49	3·67	2·97
Histidine	0·84	2·45	0·09	0·64
Lysine	3·34	8·02	2·23	4·06
Aspartoyl	10·44	10·00		9·50
Glutamic acid	11·27	15·61	11·62	16·15
Proline	11·48	3·32	1·61	11·47
Hydroxyproline			20·0	
Free amino acid	—	1·98		—

where θ_0 is the inherent contact angle of the surface substance and r_a is the ratio of the actual surface area to the projected surface area of the corrugated surface. From Eqn (5), θ_a is larger than θ_0 for the body surfaces of soil animals because the inherent contact angle of water on their body surfaces is over 90°. It was concluded that the geometrically non-smooth morphology of soil animals would enhance their inherent hydrophobicity. In addition, when the absolute value of the tilt angle α is more than $(180–\theta_0)$, a composite interface would be formed and air would be intercepted in the troughs. The larger was the absolute value of α, the larger θ_a.

If the rough morphology of body surfaces of soil animals are molecular fractals, the apparent contact angles of water on the fractal rough surfaces are also larger than their inherent contact angles according to the wettability analysis of molecular fractal surfaces by Hazlett (1990). In this case, the inherent hydrophobicity of body surfaces of soil animals would be enhanced as the molecular fractal dimensions are increased.

Solid surfaces on which contact angles of water are higher have, in most cases, lower soil adhesion. As they can enhance their inherent hydrophobic ability, the microscopic geometrically non-smooth structure of the body surfaces of soil animals is a surface morphology beneficially reducing the soil adhesion to their body surfaces. The macroscopic non-smooth structure existing

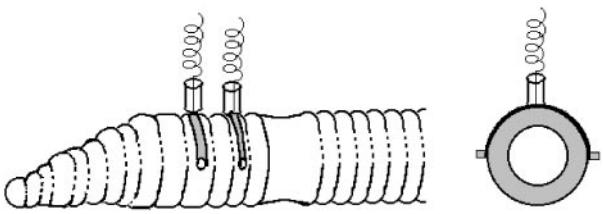

Fig. 8. Schematic diagram showing a method for measuring surface electric potential of earthworm body (Sun et al., 1991)

Table 4
Mean and maximum values of the surface electric potential of earthworm *Michaelsen* body tissue (Sun *et al.*, 1991)

	Electric potential of Michaelsen when creeping, mV		*Electric potential of Michaelsen through a tube, mV*	
Position on body	*Maximum*	*Mean*	*Maximum*	*Mean*
Fore part	40	21	35	20
Middle part	30	11	19	9
Hind part	18	11	18	5

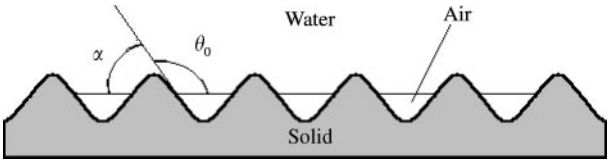

Fig. 9. Schematic diagram for the corrugated surface profile of soil-borrowing animals (Tong et al., 1994d)

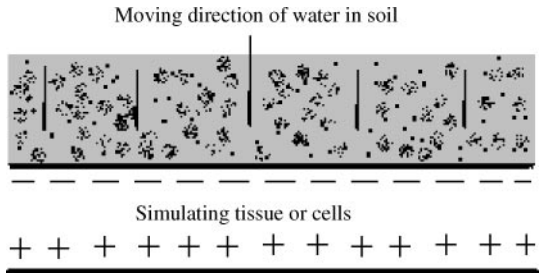

Fig. 10. Schematic diagram of the microscopic electro-osmotic system existing on the body surface of soil animals in contact with soil

on the body surfaces of soil animals can decrease the actual contact area of their body surface with soil and change the contact state, so that the soil adhesion and resistance to motion can be reduced.

Ren *et al.* (1990b) analysed the effects of the claw configuration of soil animals on the anti-adhesive characteristics. It was considered that the soil dug by the claws of the soil animals cannot stick to, and easily slides along, the claw surfaces owing to the increase in the upward curvature of claw surfaces from the claw tip.

4.2. *Hydrophobicity*

It was found that the water film on the body surfaces of soil animals would rapidly contract and fall from their bodies as they came out of wet soil. This phenomenon indicated that their body surfaces had a strong hydrophobic nature. The organic substances, similar to resin and paint, including hydrophobic membranous protein and non-polar radicals of phospholipid on the body surfaces contributed to their hydrophobic nature. The hydrophobic ability of the body surfaces suggested that the attraction between the body surface substances and water molecules was very weak. It can be considered that the body surface substances were low surface energy materials. The inherent hydrophobic ability of the body surfaces of soil animals would be enhanced by their geometrically non-smooth or rough structure. The combination of the geometrically non-smooth structure and its hydrophobic nature is even better in preventing soil from sticking to the body surfaces of soil animals.

4.3. *Microscopic electro-osmosis*

The action potential can be induced by stimulating the body parts of soil animals. When soil animals are in contact with the soil, a microscopic electro-osmotic system would be formed in between the stimulated body parts and other parts nearby (*Fig. 10*). As a result, water in the adjacent soil moves to the contact zones owing to the action of the potential difference, the water film at the contact interfaces becomes thicker, so that the soil adhesion to the body surfaces would be reduced through lubrication. Although the amplitude of the action potential of soil animals is small, a microscopic electro-osmotic system can be formed because the distance between the positive pole and the negative pole is very short. The zone of negative polarity produced by stimulation from the contacting soil is on the same surface as the resting body part near to the stimulating zone. For example, the positive pole and the negative pole were on the segments near to each other. The action potential of the body surfaces of soil animals has a dynamic distribution feature. Therefore, this electro-osmosis was called non-smooth surface electro-osmosis (Cong *et al.*, 1995a). In addition, the action potential would stimulate such soil animals as earthworms to produce more secretions.

4.4. *Lubrication*

Li *et al.* (1990) analysed the effect of the secretion of earthworms upon its anti-adhesive characteristics. The mucoprotein as the main solute in the secretion had an open and flat construction, giving a low tangential viscous drag. As the earthworm moved through the soil, some of the secreted liquid would infiltrate into a layer of the contacting soil to form a three-layer system, *i.e.* the body surface layer, the secretion layer and the soil layer infiltrated with the secretion (*Fig. 11*). The sliding interface of the earthworm body surface against the soil occurred in the layer of the secretion near the soil layer, since the liquid provided a weak shear layer. The lubrication phenomenon of the secretion of earthworms contributed to the reduction of soil adhesion to its body.

4.5. *Flexibility*

Ren *et al.* (1998) examined the vole fur for anti-adhesive and anti-frictional characteristics. Immediately after removing the skin from a freshly killed vole, soil adhesion tests were conducted in white clay with moisture contents of 34 and 45% d.b., respectively. The soil adhesion to the

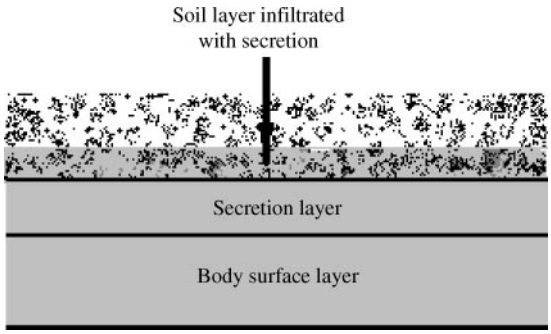

Fig. 11. Schematic diagram of a three-layer contact system between the soil and body surface of soil animals which secrete liquid substances

vole skin was measured by comparison with that for steel-45 [*Fig. 12*(*a*)] and found to be considerably less. It was observed that the vole fur was progressively separated from the soil surface during the separating procedure of the adhesion tests, emphasizing the importance of the flexible feature of the fur. Friction tests of the vole fur against soil were conducted at a sliding velocity of 0·1 m s^{-1}. The sliding direction of soil was along the growing direction of the vole fur on the body. It was shown that the sliding resistance was reduced by about 20% by comparison with steel-45 [*Fig. 12*(*b*)].

5. Biomimetics of soil-engaging components

5.1. *Components with biomimetic non-smooth surfaces*

5.1.1. *Bulldozing blades with biomimetic, embossed surfaces*

Ren *et al.* (1995c) imitated the surface morphology of the 'bulldozing blade' of the dung beetle to design and test 22 biomimetic, embossed, bulldozing blades on the pseudovariable approximation design optimizing method. The biomimetic bulldozing blades were made from a plain carbon steel and were 400 mm long by 200 mm wide. There were two arrangement patterns, a rectangle and a parallelogram (*Fig. 13*). The small convex domes embossed on the surface were 2–8 mm in height, 16–32 mm in base diameter and 20–50 in number. Bulldozing tests were conducted in an indoor soil bin using a clay soil with an average moisture content of 27·8% d.b. It was found that the bulldozing resistance of the embossed blades was reduced, on an average, by 13·02% in comparison to a conventional (smooth) blade. The structural parameters of the optimum embossed surface were convex domes, 7 mm in height, 25 mm in base diameter and 45 in number, with a parallelogram arrangement. In the optimum case, bulldozing resistance was reduced by 18·09% as compared to that of the conventional smooth blade.

Qaisrani *et al.* (1993) and Qaisrani (1993) designed embossed, bulldozing blades with six arrangement patterns (*Fig. 14*). The small convex domes were made from steel-45 and ultra high molecular weight polyethylene (UHMWPE). The small convex domes, prepared in advance, were glued on a conventional smooth steel-45 plate of 250 mm in length and 130 mm in width. The tests were conducted on a soil cutting test table. The depth and the angle of cut were 15 mm and 35°, respectively. The cutting speeds were 0·01, 0·02 and 0·06 m s^{-1}, respectively. It was found that the bulldozing resistance of the six biomimetic non-smooth bulldozing blades whose convex domes were made from UHMWPE was reduced to different extents and the fifth blade (*Fig. 14*) had the lowest resistance, which was reduced by 27·50, 28·59 and 34·0% at the cutting speeds of 0·01, 0·02 and 0·06 m s^{-1},

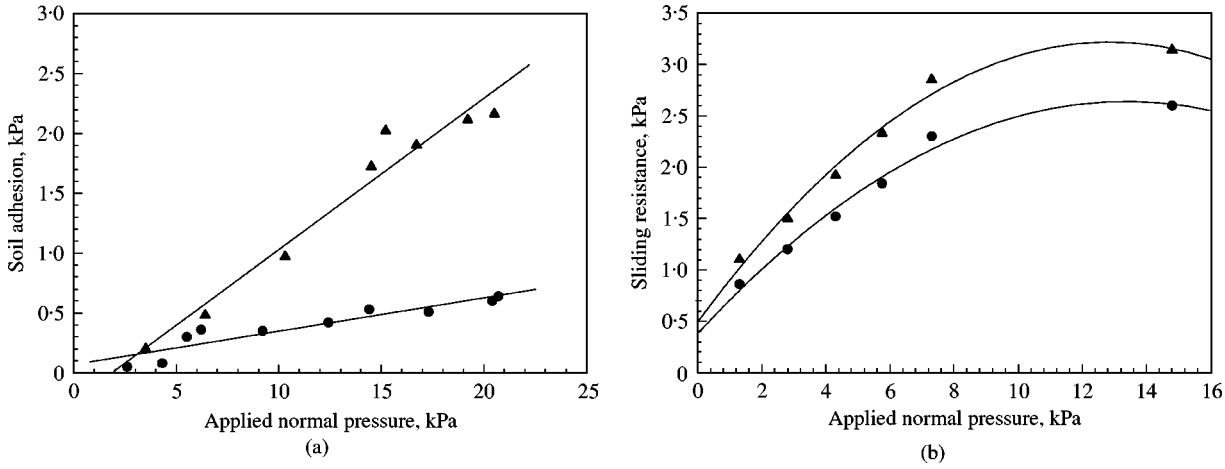

Fig. 12. Adhesion (a) and sliding resistance (b) of soil versus applied normal stress, showing better anti-adhesive and anti-frictional characteristics of vole fur (Ren et al., 1998); ▲, steel-45; —●—, vole fur

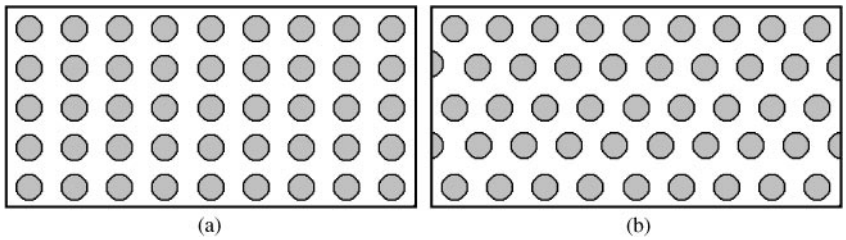

Fig. 13. Schematic diagrams showing two regular distributions of convex domes on the biomimetic embossed non-smooth bulldozing blades: (a) rectangle distribution; (b) parallelogram (Ren et al., 1995c)

respectively. Of the six bulldozing blades whose convex domes were made from steel-45, the fifth blade was the only blade with a reduction in the bulldozing resistance, which was reduced by 1·3, 1·5 and 15·55% at the cutting speed of 0·01, 0·02 and 0·06 m s^{-1}, respectively. The resistance of the other blades was higher than that of the conventional blade.

Li *et al.* (1995) conducted a statistical analysis of the characteristic parameters of the surface morphology of the 'bulldozing blades' of the dung beetle, including the characteristic dimensions, and the number of the small convex domes, using a scanning electron microscopy photograph. It was found that the position distribution of the small convex domes on the 'bulldozing blade' surface followed a statistically uniform distribution because the number of the convex domes N_L through a straight line segment along any direction was in direct proportion to the length L of this segment, that is,

$$N_L = a + bL \tag{6}$$

where a and b were parameters to be estimated, which were $-0{\cdot}2430$ and 0·1692, respectively, for the dung beetle tested. The base diameter of the convex domes ranged from 0·033 to 0·749 mm. The size of the base diameter of the convex domes followed a Gaussian distribution on the basis of the χ^2 test and the mean and the root-mean square deviation were 0·052 and 0·008 mm, respectively.

Based on the above statistical analysis, a biomimetic embossed bulldozing blade was designed by Ren *et al.* (1995b) (*Fig. 15*). The blade and the convex domes were made from a plain low carbon steel (Q235A). The tests were run on a soil cutting test table using a clay soil with a moisture constant of 27% d.b. at the angle of cut of

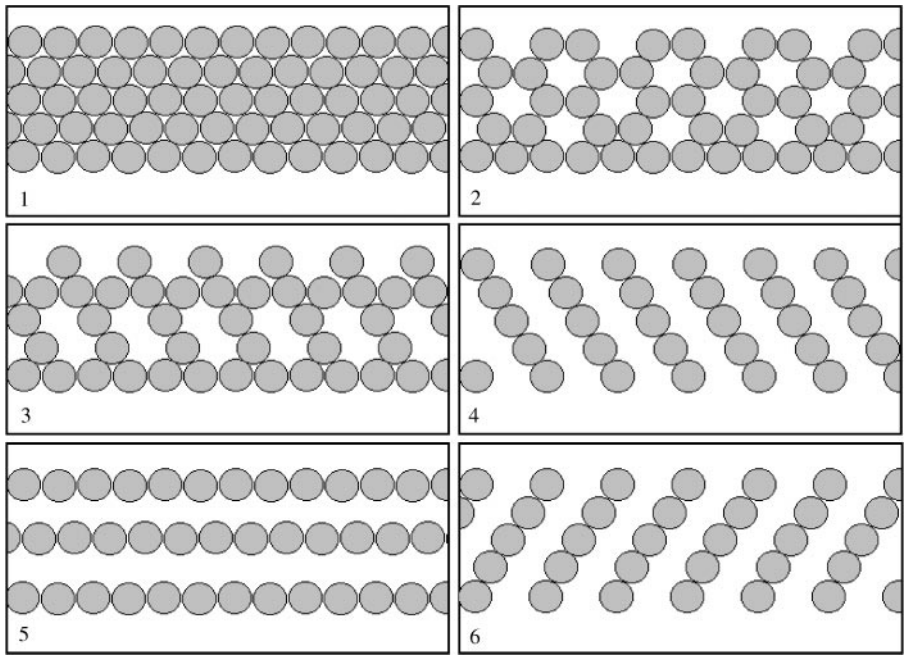

Fig. 14. Schematic diagrams showing six regular distribution patterns of convex domes on biomimetic embossed non-smooth bulldozing blades (Qaisrani, 1993)

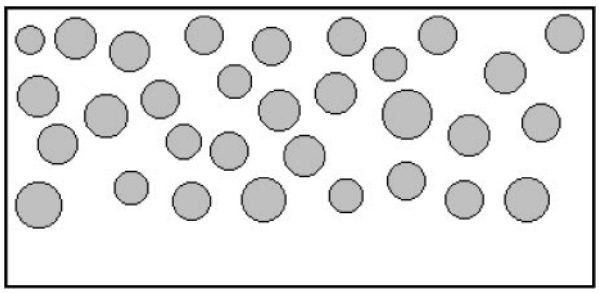

Fig. 15. Schematic diagram of a biomimetic embossed non-smooth bulldozing blade with a random distribution of small convex domes (Li et al., 1995; Ren et al., 1995b)

31–46° (the angle of the blade with respect to the direction of travel in the horizontal plane) and the cutting speeds of 13·33–58·82 mm s^{-1}. It was demonstrated that the biomimetic blade had a lower resistance to forward travel (*Fig. 16*).

5.1.2. *Bulldozing blades with biomimetic, corrugated surfaces*

Cong *et al.* (1996) imitated the wavy structure of body surfaces of some soil animals and designed a biomimetic, corrugated bulldozing blade (*Fig. 17*). The dimensions of the biomimetic blades prepared were 300 mm long by 150 mm wide. Six biomimetic blades of different wave parameters were prepared and cutting tests demonstrated that the soil adhesion to the conventional blade did not occur on the corrugated blade. The bulldozing resistance of the biomimetic, corrugated blade was reduced considerably in comparison with the conventional blade. Chen *et al.* (1996) conducted finite element analysis of the interaction between the soil and a corrugated

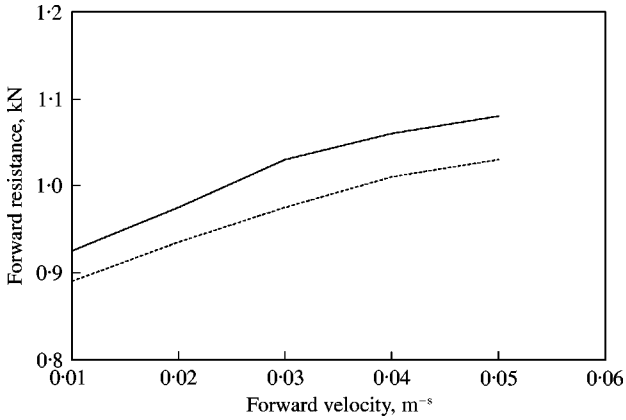

Fig. 16. Forward resistance versus forward velocity, showing a reduced resistance for the biomimetic embossed non-smooth bulldozing blade with a random distribution of convex domes compared with a conventional blade (Ren et al., 1995b); ------, biomimetic blade; ——, conventional blade

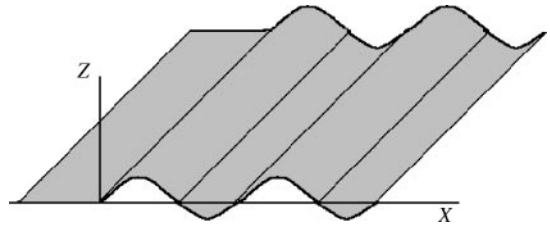

Fig. 17. Schematic diagram of biomimetic corrugated non-smooth bulldozing blade (Cong et al., 1996)

bulldozing blade and predicted the horizontal and vertical components of the bulldozing resistance during operation.

5.1.3. *Bulldozing blades with biomimetic dimpled and scaly surfaces*

Cong *et al.* (1995b) designed biomimetic, non-smooth bulldozing blades imitating the dimpled form and the scaly form of surfaces of soil animals (*Fig. 18*). A comparative test of the bulldozing resistance of the two biomimetic bulldozing blades in clay soil, wet sand and dried sand was conducted. It was found that the resistance against wet sand and dried sand was increased markedly, while the resistance in a disturbed yellow clay was reduced considerably.

5.1.4. *Mouldboard ploughs with biomimetic embossed surfaces*

Qaisrani *et al.* (1992) designed a biomimetic, embossed plough mouldboard. It was prepared by gluing small convex domes on the surface of a conventional mouldboard (steel-35). The small convex domes had a base diameter of 20 mm and a height of 2 mm and were made from UHMWPE. Suminitrado *et al.* (1988) concluded that the angles of the sliding direction of the soil on the mouldboard surface with the horizontal surface was between 55 and 65°. Based on this phenomenon, an arrangement pattern of convex domes on the mouldboard was designed (*Fig. 19*). The biomimetic plough was tested in an indoor soil bin using black clay soil. The ploughing resistance of this biomimetic non-smooth plough was reduced by 26 and 34% at the forward speeds of 3·6 and 5·0 km h^{-1}, respectively, as compared with a corresponding smooth mouldboard plough. The soil adhering to the biomimetic plough surface was less than that to the smooth plough.

Li *et al.* (1996a) designed a biomimetic, embossed mouldboard plough with the same non-smooth structure as the biomimetic bulldozing blade surface shown in *Fig. 15*, namely, the base diameter of small convex domes on the mouldboard surface was a Gaussian distribution and the position of the convex domes was a statistically

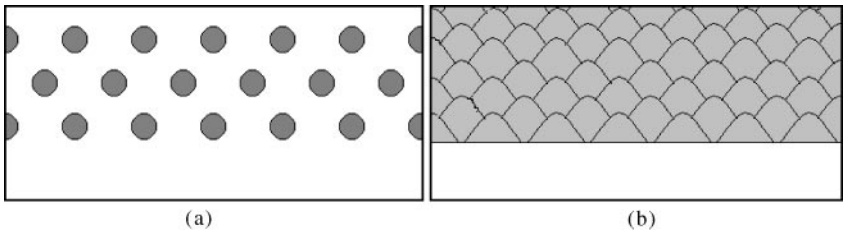

Fig. 18. Schematic diagram of the biomimetic bulldozing blades: (a) dimpled, and (b) scaly (Cong et al., 1995b)

uniform distribution. The material from which the convex domes were made was a white iron alloy possessing a better anti-adhesive characteristic (Li, 1993). The white iron alloy was manufactured into a metal pencil. The convex domes on the mouldboard were prepared through weld accumulation on the white iron alloy of a conventional mouldboard made from steel-35. It was demonstrated that the resistance of the biomimetic plough was reduced by 6·6–12·7% as compared to the corresponding conventional mouldboard plough.

5.2. *Modification of soil-engaging materials*

5.2.1. *Iron and steel*

Chen *et al.* (1995a) examined the effects of the chemical composition and microstructures on the water wettability, corrosion resistance and soil-scouring properties of three materials traditionally used for cast-iron mouldboards in China. The mouldboards made in Yangcheng in Shanxi province of China had the best soil scouring property of the three traditional mouldboards. Its typical composition featured higher carbon and phosphorus and lower manganese, silicon and sulphur content. A representative composition by weight of the mouldboard included carbon of 4·27%, phosphorus of 0·58%, manganese of 0·07%, silicon of 0·05% and sulphur of 0·032%. It was also found that the Yangcheng mouldboard material had the best corrosion resistance. Li *et al.* (1996b) tested the effect of the corrosion resistance of steel-35 on its anti-adhesive characteristic to soil. The microstructure of steel-35, hardened and tempered at a low temperature or hardened and tempered at a high temperature, had higher corrosion resistance than that for the microstructure hardened and tempered at an average temperature, as did their anti-adhesive characteristic to soil. The soil adhesion to iron and steel was related to their individual relative surface potential. A calomel electrode was taken as a standard electrode for comparison to determine the relative surface potentials of steel-35 of different microstructures using 0·1% NaCl solution as electrolyte (Li *et al.*, 1997). The soil adhesion to steel-35 with a microstructure of a lower relative surface potential was lower (*Fig. 20*). This phenomenon seems to have a corresponding relation with the characteristic phenomenon of the action potential of soil animals.

Li (1993) developed a white iron alloy and applied it for preparing convex domes for the embossed surfaces. The white iron alloy had a lower relative surface potential. In addition, the iron had a better abrasion resistance. The biomimetic, embossed plough whose convex domes on the mouldboard were made from the iron displayed

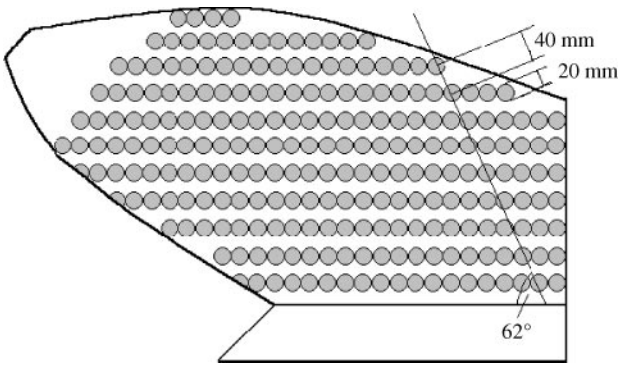

Fig. 19. Schematic diagram of a biomimetic mouldboard plough (Qaisrani et al., 1992)

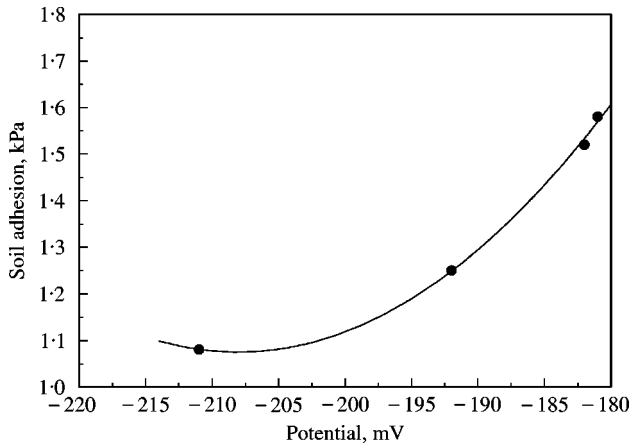

Fig. 20. Soil adhesion to steel-35 versus its surface relative potential (Li et al., 1997)

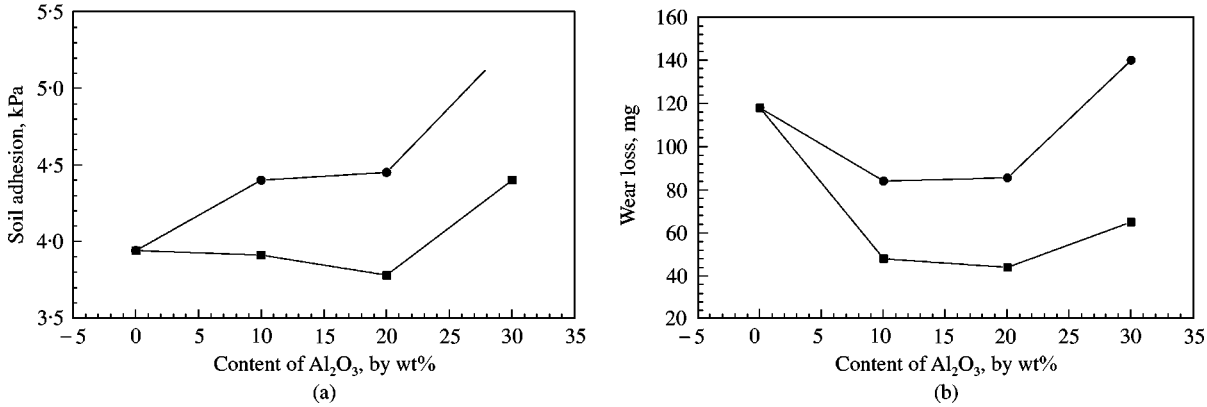

Fig. 21. Effects of size and content of Al_2O_3 particles on the polytetrafluoroethylene (PTFE) matrix composite reinforced with Al_2O_3 particles: (a) soil adhesion; (b) abrasive wear; —■—, 120 mesh; —●—, 280 mesh (Lu et al., 1996)

a better anti-adhesion characteristic and lower ploughing resistance (Li *et al.*, 1996a).

5.2.2. *Polymer composites and coatings*

Although they had a better anti-adhesive characteristic, applications of polymeric materials to soil-engaging components were limited because of their lower abrasive wear resistance against soil (Tong *et al.*, 1994b, 1999; Chen *et al.*, 1994). The composite material technique is a better method for increasing abrasive wear resistance of polymeric materials. The second phase particles or fibres existing in composite materials can make their surfaces possess a feature similar to the geometrically non-smooth topography of the body surfaces of soil animals.

Tong *et al.* (1990b) and Lu *et al.* (1996) prepared an alumina particle reinforced Teflon composite material. When the alumina particle content was less than 20% by weight, its abrasive wear resistance was increased considerably and the soil adhesion was affected a little (*Fig. 21*). Liu *et al.* (1998a, 1998b) tested the effects of quartz particles and glass beads as the reinforced materials upon soil adhesion and abrasive wear of UHMWPE. The anti-adhesive characteristic of the UHMWPE matrix composite was little affected, as long as the volume content of the reinforced materials in the composite was not more than 9% by volume.

Jia *et al.* (1993) analysed the water wettability of composite materials reinforced with particles. Based on the assumption that (a) the particles in composite materials were spherical and had the same diameter which was smaller than the water droplet during tests of contact angles of water on the surfaces of composites, (b) the particles were uniformly distributed in the matrix of the composite materials, and (c) the outer surfaces of particles were circular with variable diameters, they derived a theoretical equation for the particle reinforced composite materials as follows:

$$\cos\theta_c = \cos\theta_1 + \frac{3\sqrt{2}}{4} V(\cos\theta_2 - \cos\theta_1) \qquad (7)$$

where: θ_c is the contact angle of water on the surfaces of a composite material; θ_1 is the inherent contact angle of water on the matrix material; θ_2 is the inherent contact angle of water on the reinforcing material in bulk; and V is the volume content of reinforcing particles in a composite material. The contact angles of water on nylon 1010 (PA1010) composite materials reinforced with alumina particles followed Eqn (7).

Jia *et al.* (1995a, 1996a, 1996b, 1996c) prepared the alumina particle reinforced PA1010, epoxy (EP), polyurethane (PU) matrix composite coatings and the steel-T8 coating impregnated with polysiloxane. These coatings were applied to a smooth bulldozing blade and/or the fifth embossed blade shown in *Fig. 14* and tested for their bulldozing resistance in a soil cutting test table using clay soil with moisture contents of 29·4 and 33·0% d.b. The cutting speed was 0·02 and 0·04 m s^{-1}, the depth of cut was 20 mm and the angle of cut was 45°. In the comparison with an uncoated smooth blade, the reductions in cutting resistance were 26·38, 23·23 and 22·27% for the smooth bulldozing blades coated with PA1010, EP and steel-T8 coatings, respectively, and 23·58 and 35·20% for the non-smooth bulldozing blades coated with PA1010 and PU composite coatings, respectively. After EP and PA1010 composite coatings were applied to the plough mouldboards, their ploughing resistance was reduced by 30·31 and 35·88%, respectively, and no soil stuck to the mouldboard as compared to the conventional one (steel-35). The soil used for the test was black clay with a moisture content of 20·5% d.b. Both depth and width of the plough were 200 mm. The

forward speed was 0·95–1·88 m s^{-1}. The above results showed that the combination of hydrophobic materials and geometrically non-smooth surfaces was a better method for reducing adhesion and interfacial friction of soil-engaging components.

5.3. *Biomimetic non-smooth electro-osmosis*

5.3.1. *The basic structure of biomimetic electro-osmotic surfaces*

Based on the characteristics of the surface action potential of soil animals, a combined measuring dome was designed (*Fig. 22*) by Cong *et al.* (1995a) with a positive pole in the centre and a negative pole at the periphery. This combined disc was used for testing, in principle, the effect of the electro-osmosis upon soil adhesion. The soil used had a moisture content of 23·5% d.b. The voltage for electro-osmotic tests was 12 V. The applied normal stress was 26·78 kPa. It was found that there existed an area ratio for the zones of positive and negative polarities that resulted in minimum soil adhesion. In other words, the ratio of the area of positive pole to negative pole was an important factor affecting soil adhesion. This electro-osmotic system in which the positive pole and negative pole were on the same surface and the positive pole was on a convex dome was called non-smooth surface electro-osmosis or biomimetic electro-osmosis.

5.3.2. *Bulldozing blades with biomimetic electro-osmosis*

According to the principal test results, Cong *et al.* (1995a), Ren *et al.* (1995a) designed two biomimetic bulldozing blades with non-smooth surface electro-osmotic structures. One was the convex dome positive pole [*Fig. 23*(*a*)] and another was the corrugated form of the positive pole [*Fig. 23*(*b*)]. Bulldozing tests were conducted on a soil cutting test table. The forward speed was from 43 to 172 mm s^{-1}, the depth cut was 50 mm, the angle of cut was 60°, the voltage for electro-osmosis was 12 V and the ratio of area of the positive pole to the negative pole was 1 : 7·3. It was found that when soil stuck on the surface of the conventional blade and the non-smooth surface without electro-osmosis, only a little or no soil stuck to the surface of biomimetic, electro-osmotic plate under identical conditions. Biomimetic electro-osmosis can further reduce bulldozing resistance by 9–12% and 15–32% for the embossed and for the corrugated non-smooth surfaces, respectively, as compared with the corresponding non-smooth surface without electro-osmosis.

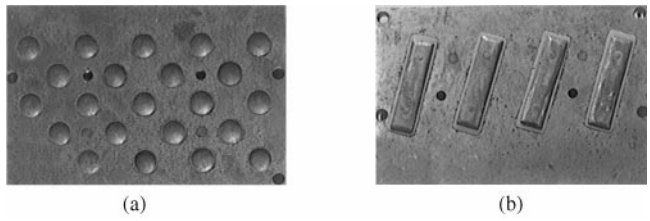

Fig. 23. Photographs of two biomimetic bulldozing blades with electro-osmosis: (a) embossed; and (b) corrugated (Ren et al., 1995a)

5.3.3. *Wheel lugs with biomimetic electro-osmosis*

The electro-osmotic principle for non-smooth surfaces was used by Chen *et al.* (1995b) for the lugs of paddy-field wheels. They designed varied convex forms of biomimetic lugs (*Fig. 24*). The tests were conducted in an indoor soil bin using supersaturated black clay soil similar to that found in paddy fields. The working depth of lugs was 150 mm. Soil blockage due to adhesion occurred on the conventional lugs without electro-osmosis and the blocked soil was not self-cleaning, while only a little soil adhered to the lugs with biomimetic electro-osmosis and the lugs were self-cleaning. When a voltage of 24 V was used for electro-osmosis and convex domes with a base diameter of 24 mm were taken as positive poles, the soil shedding property of lugs was the best at an area ratio for the zones of positive and negative polarity of 8–12·5%. The traction force and the driving efficiency of

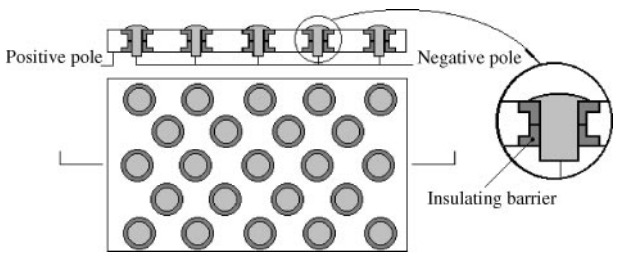

Fig. 22. Schematic diagram of a biomimetic bulldozing blade with an embossed non-smooth surface structure for elecro-osmosis (Cong et al., 1995a)

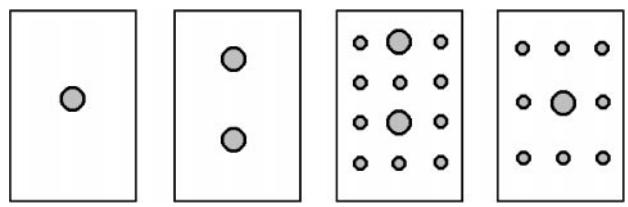

Fig. 24. Schematic diagrams of biomimetic electro-osmotic surface structures used for the lugs of paddy-field wheels (Chen et al., 1995b)

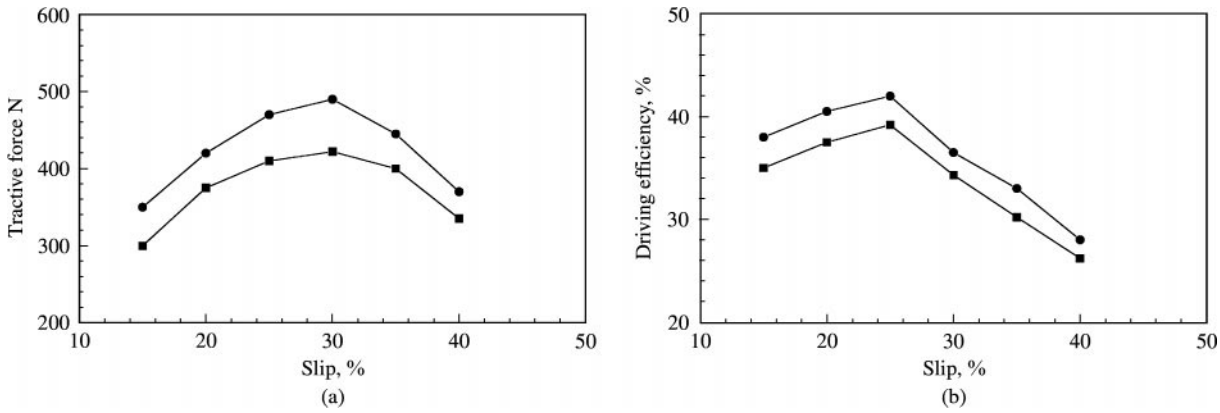

Fig. 25. Effects of biomimetic electro-osmotic lugs on a paddy-field wheel: (a) tractive force, (b) tractive efficiency (Chen et al., 1995b); —●—, with electro-osmosis; —■—, without electro-osmosis

paddy-field wheels were increased owing to biomimetic electro-osmosis (*Fig. 25*).

5.4. *Flexible components for removing soil*

5.4.1. *Loading bucket with a flexible lining*

Sun *et al.* (1992, 1996a, 1996b) designed a flexible steel mesh based on the flexibility features of soil-burrowing animals. The steel mesh was made from linked steel rings and slotted steel rings [*Fig. 26*]. The steel mesh was made into a lining suitable for such soil-engaging components as digger buckets and wheel buckets. The position of the lining could be changed with the position of the bucket as shown in *Fig. 27*. When the bucket with a steel mesh lining was filled with soil, the lining was pressed close to the inside of the bucket. At the beginning of unloading, both soil and the lining slid out from the bucket simultaneously, and then the soil was separated from the lining gradually by gravity and, finally, the lining was hung from the bucket. Only the smaller size of soil particles could enter between the lining and the inside of the bucket through the gap in the lining, since the size of the gaps in the lining was very small. In order to protect soil from blocking between the lining and the inside of the bucket, several holes were drilled through the bottom of the bucket shell to release the trapped soil.

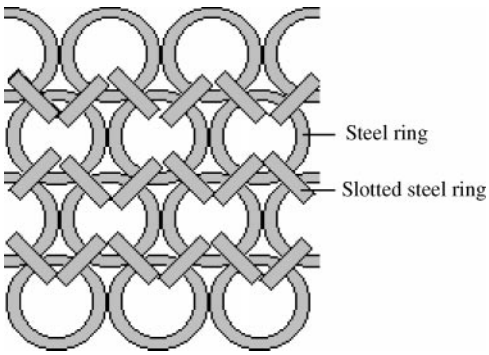

Fig. 26. Schematic diagram of structure of a flexible steel mesh lining (Sun et al., 1992)

5.4.2. *Self-unloading box of dump truck with flexible chains*

Wang *et al.* (1997) tested the effect of three flexible linings, steel mesh, steel chain and nylon-knitted net, on a model of a self-unloading box. The tests were conducted using yellow clay with a moisture content of 24·5% d.b. After 20 successively loading–unloading operations, the soil adhering to the box without flexible lining was 14% by volume of the total holding capacity of the box. Heavy soil adhesion took place after 10 loading–unloading operations for the nylon-knitted net and, afterwards, it lost the flexible function and soil-shedding action. The nylon-knitted net was found to be broken easily. No soil was built up on the steel mesh lining and the steel chain lining after 20 loading–unloading operations. The steel mesh lining and the steel chain lining would increase the deadweight of the self-unloading box, which is their disadvantage.

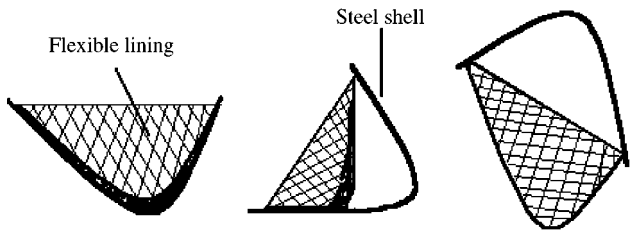

Fig. 27. The position of the flexible lining with respect to the bucket (Sun et al., 1996b)

6. Summary

The phenomenon of soil adhesion existing between soil and the soil-engaging surfaces of varied terrain machines increases their working resistance and energy consumption and decreases their quality of work. The adhesion results from the capillary pressure and the viscous resistance of the water film at the interface for wet soil, was mainly due to the molecular attraction and the negative air pressure for dry soil. The factors affecting soil adhesion include the nature and properties of the soil, the properties of the soil-engaging component surfaces and the experimental conditions. The conventional methods for reducing soil adhesion include the design of surface shapes, selection of surface materials for soil-engaging components and application of electro-osmosis, magnetic fields, vibration and lubrication.

Soil-burrowing animals have significant anti-adhesive characteristics through evolution over millions of years. The reasons why the body surfaces of soil-burrowing animals do not stick to soil includes varieties of geometrically non-smooth morphologies, chemical composition and hydrophobicity, microscopic electro-osmotic systems formed by their bioelectricity and flexibility of their body surfaces and the lubrication action of the liquid substances on their body surfaces as well. Various biomimetic methods were developed on the basis of the anti-adhesive principles of soil-burrowing animals. These biomimetic methods were the development of non-smooth surfaces for soil-engaging surfaces, electro-osmotic systems, and flexible parts for removing soil accretion on the soil-engaging components.

Acknowledgements

This project was supported by the National Natural Science Foundation of China (Grant No. 59835200) and Doctoral Foundation of China (Grant No. 97018514).

References

Adamson A W (1976). Physical Chemistry of Surfaces (3rd Edn). Interscience, New York

Akiyama Y; Yokoi O (1972a). Study on soil adhesion. Part II. Theoretical analysis of adhesion mechanism at the saturation stage. Journal of Japanese Soil Fertilizer Science, **43**(8), 271–277

Akiyama Y; Yokoi O (1972b). Study on soil adhesion. Part III. Theoretical analysis of adhesion mechanism at the water loop linking stage. Journal of Japanese Soil Fertilizer Science, **43**(9), 315–320

Araya K; Kawanishi K (1984). Soil failure by introduction air under pressure. Transactions of the ASAE, **27**(5), 1292–1297

Avnir D; Farin D; Pfeifer P (1985). Surface geometric irregularity of particulate materials: the fractal approach. Journal of Colloid and Interface Science, **103**(1), 112–123

Bowden F P; Tabor D (1954). The Friction and Lubrication of Solids. Clarendon Press, Oxford

Chancellor W J (1994). Friction between soil and equipment materials—review. ASAE Paper, No. 94-1034

Chen B; Ren L; Li A; Hu Q (1990a). Study on the method of collecting the body surface liquid of earthworms. Transactions of the Chinese Society of Agricultural Engineering, **6**(2), 7–12

Chen B; Ren L; Xu X; Cui X; Wang Y; Zhang B; Ge L; Jin G (1990b). Research on reducing soil adhesion of body surfaces of typical soil animals. Transactions of the Chinese Society of Agricultural Engineering, **6**(2), 1–6

Chen B; Li J; Ren L (1995a). Research on scouring soil for materials of the traditional plow moldboard. Transactions of the Chinese Society Agricultural Machinery, **26**(1), 46–49

Chen B; Liu D; Ning S; Cong Q (1995b). Research on the reducing adhesion and scouring of soil of lugs by using unsmoothed surface electro-osmosis method. Transactions of the Chinese Society of Agricultural Engineering, **11**(3), 29–33

Chen B; Wang G; Ren L (1996). Finite element analysis on the interaction between soil and unsmoothed surface. In: Proceedings of the 12th International Conference of ISTVS, 7–10 October (Yu Q; Qiu L, eds), pp 89–95. Beijing, People's Republic of China

Chen Y; Tong J; Ren L; Chen B (1994). Abrasive wear behavior of several soil adhesion-reducing materials. Transactions of the Chinese Society of Agricultural Engineering, **10**(Suppl), 91–95

Clyma H E; Larson D L (1991). Evaluating the effectiveness of electro-osmosis in reducing tillage draft force. ASAE Paper No. 91-3533

Cong Q; Ren L; Chen B (1990a). Research on reducing adhesion results of soil electro-osmosis and its affecting factors. In: Proceedings of the 10th International Conference of the ISTVS, 20–24 August, pp 45–55, Kobe, Japan

Cong Q; Ren L; Chen B; Su F (1990b). A study on adhesion-reducing methods of terrain-machine. Transactions of the Chinese Society of Agricultural Engineering, **6**(1), 8–14

Cong Q; Ren L; Wu L; Chen B; Li A; Hu A (1992). Taxonomic research on geometric non-smooth animal surface shapes. Transactions of the Chinese Society of Agricultural Engineering, **8**(2), 7–12

Cong Q; Wu L; Ren L; Chen B (1995a). The principled experiment of reducing soil adhesion and scouring soil by non-smooth surface electro-osmosis. Transactions of the Chinese Society of Agricultural Engineering, **11**(3), 19–23

Cong Q; Ren L; Wang G; Chen B (1995b). Study on the reduction of soil adhesion and resistance about bionic non-smooth surface by test. In: Proceedings of the International Conference of Agricultural Mechanization, 10–13 April, pp 33–39, Beijing, People's Republic of China

Cong Q; Wang L; Ren L; Chen B; Zhou S; Li A (1996). Biomimetic bulldozing plates with wave-form non-smooth surfaces for reducing soil adhesion and resistance. Construction Machinery (China), (3), 28–30

Cui X; Zhang N; Wang Y; Ren L; Xu X; Chen B; Li A (1990). Constitution of pangolin scales and mechanism of reducing adhesion of soil to their cuticle. Transactions of the Chinese Society of Agricultural Engineering, **6**(3), 15–22

Fountaine E R (1954). Investigation into the mechanism of soil adhesion. Journal of Soil Science, **5**(2), 251–263

Fox W R; Bockhup C W (1965). Characteristics of a Teflon-covered simple tillage tool. Transactions of the ASAE, **8**(2), 227–229

Gill W R; Vanden Berg G E (1967). Soil Dynamics in Tillage and Traction. Agricultural Handbook, No. 316. Agricultural Research Service. US Department of Agriculture

Guo P; Liu J (1995). The effect of magnetized plowshare upon tillage performance. Agricultural Research in the Arid Areas (China), **13**(2), 103–109

Han G; Zhang Y (1991). Measurement and analysis of ploughing resistance on the magnetic plough. Transactions of the Chinese Society Agricultural Machinery, **22**(3), 25–28

Hazlett T D (1990). Fractal applications: wettability and contact angle. Journal of Colloid and Interface Science, **137**(2), 527–533

Hendrick J G; Bailey A C (1982). Determining components of soil-metal sliding resistance. Transactions of the ASAE, **25**(4), 845–849

Jia X; Ren L; Chen B (1995a). Characteristics of reducing adhesion and resistance of bionic coatings prepared for touching-soil components of terrain machinery. Transactions of the Chinese Society of Agricultural Engineering, **11**(4), 10–13

Jia X; Ren L; Chen B; Tong J; Cong Q (1995b). Affects of soil animal's unsmoothed cuticles on the wettability of the cuticles. Transactions of the Chinese Society of Agricultural Engineering, **11**(4), 1–4

Jia X; Ren L; Chen B (1996a). Wettability of unsmoothed surfaces of soil animals' cuticles and bionic composite coatings. Chinese Journal of Materials Research, **10**(5), 556–560

Jia X; Ren L; Chen B (1996b). Characteristics of bionic composite coating reducing adhesion and resistance. Chinese Journal of Materials Research, **10**(2), 210–214

Jia X; Ren L; Chen B (1996c). The functions of reducing adhesion and resistance of PA1010, EP composite coatings and surface improved moldboards. Transactions of the Chinese Society of Agricultural Machinery, **27**(3), 7–11

Jia X; Ren L; Tong J; Chen B (1993). Wettability of chemical unsmoothed surfaces and rough surfaces. Transactions of the Chinese Society of Agricultural Engineering, **9**(3), 9–13

Li J (1993). A study on the bionic plow moldboard of reducing soil adhesion and plowing resistance. PhD Thesis, pp 77–93, Jilin University of Technology, Changchun, China

Li J; Jiang M; Li Y (1997). The relationship between soil adhesion and surface potential of steel. Transactions of the Chinese Society of Agricultural Engineering, **13**(2), 42–45

Li A; Ren L; Chen B; Cui X (1990). Constitution and mechanism analysis of reducing soil adhesion for the body surface liquid of earthworms. Transactions of the Chinese Society of Agricultural Engineering, **6**(3), 7–14

Li J; Ren L; Chen B; Gu W (1993a). A study on the soil adhesion characteristics of 35 steel. Transactions of the Chinese Society of Agricultural Engineering, **9**(2), 19–25

Li J; Ren L; Chen B; Gu W (1993b). The effect of microstructure of steel on soil adhesion characteristics. Transactions of the Chinese Society of Agricultural Engineering, **9**(3), 14–21

Li J; Ren L; Chen B (1995). The statistics analysis and mathematical analogy of the unsmoothed geometrical units on the surface of soil animal. Transactions of the Chinese Society of Agricultural Engineering, **11**(2), 1–5

Li J; Ren L; Liu C; Chen B (1996a). A study on bionic plow moldboard of reducing soil adhesion and plowing resistance. Transactions of the Chinese Society of Agricultural Machinery, **27**(2), 1–4

Li J; Ren L; Chen B; Jiang M (1996b). Study on surface characteristics of materials of plough moldboard and their effects on soil adhesion. Transactions of the Chinese Society of Agricultural Engineering, **12**(2), 45–48

Liu C; Ren L; Tong J (1998a). Wettability and soil adhesion of glass bead reinforced UHMWPE matrix composites. Acta Materiae Compositae Sinica, **15**(2), 29–33

Liu C; Ren L; Tong J (1998b). Behavior of soil adhesion on soil-engaging components. Transactions of the Chinese Society of Agricultural Engineering, **14**(4), 37–42

Low P F (1979). Nature and properties of water in montmorillonite–water systems. Soil Science Society of America Journal, **43**(8), 651–658

Lu X; Wen S; Tong J; Chen Y; Ren L (1996). Wettability, soil adhesion, abrasion and friction wear of PTFE (+ PPS) + Al_2O_3 composites. Wear, **193**(1), 48–55

Ma J (1984). Creatures and Bionics. Tianjin Science and Technology Press, Tianjin

Mandelbrot B B (1982). The Fractal Geometry of Nature. W. H. Freeman, New York

Pfeifer P (1984). Fractal dimension as working tool for surface-roughness problem. Application of Surface Science, **18**(2), 146–164

Perfect E; Kay B D (1995). Applications of fractals in soil and tillage research: a review. Soil & Tillage Research, **36**(1), 1–20

Qaisrani A R (1993). The effects of modified and unsmoothed surfaces on the drafts of bulldozing plates and moldboard plows. PhD Thesis, pp 70–120, Jilin University of Technology, Changchun, China

Qaisrani A R; Chen B; Ren L (1992). Modified and unsmoothed plow surfaces—a means to reduce plowing resistance. International Agricultural Engineering Journal, **1**(3), 115–124

Qaisrani A R; Tong J; Ren L; Chen B (1993). The effects of unsmoothed surfaces on soil adhesion and draft of bulldozing plates. Transactions of the Chinese Society of Agricultural Engineering, **9**(1), 7–13

Ren L; Tong J; Chen B; Wu L (1990a). Thermodynamic analyses of behavior of soil–solid surface adhesion. Transactions of the Chinese Society of Agricultural Engineering, **6**(4), 7–12

Ren L; Xu X; Chen B; Cui X; Wang Y; Zhang B; Ge L; Jin G (1990b). Research on claw shapes of typical soil animals. Transactions of the Chinese Society of Agricultural Machinery, **21**(2), 44–49

Ren L; Chen D; Hu J (1990c). Initial analysis on the law of reducing adhesion of soil animals. Transactions of the Chinese Society of Agricultural Engineering, **6**(1), 15–20

Ren L; Zhang J; Chen B; Qi B (1990d). Bionics research on reducing adhesion and resistance of soil for flexible shovel. Transactions of the Chinese Society of Agricultural Machinery, **21**(4), 33–39

Ren L; Cong Q; Chen B; Wu L; Li A; Jing D (1992a). A study on the adhesion reducing character of geometric non-smooth surface of typical animal. Transactions of the Chinese Society of Agricultural Machinery, **23**(2), 29–35

Ren L; Tong J; Cong Q (1992b). Non-smooth surfaces of interfacial adhesion. In: New Technology and Application of Terrain-Vehicles and Machinery. Proceedings of the Third Asia-Pacific Conference of ISTVS, 10–13 August, pp 227–230, Changchun, People's Republic of China

Ren L; Cong Q; Wu L; Chen D (1995a). Study on the reduction of soil adhesion and resistance by the application of non-smooth surface electro-osmosis. Transactions of the Chinese Society of Agricultural Engineering, **11**(3), 24–28

Ren L; Li J; Chen B (1995b). Unsmoothed surface on reducing resistance by bionics. Chinese Science Bulletin, **40**(13), 1077–1080

Ren L; Tong J; Zhang S; Chen B (1995c). Reducing sliding resistance of soil against bulldozing plates by unsmoothed bionics surfaces. Journal of Terramechanics, **32**(6), 303–309

Ren L; Wang Y; Li J; Sun S (1996). Bionic research on flexible non-smooth surface of typical animals. Transactions of the Chinese Society of Agricultural Engineering, **12**(4), 31–36

Ren L; Wang Y; Li J; Tong J (1998). Flexible unsmoothed cuticle of soil animals and their characteristics of reducing adhesion and resistance. Chinese Science Bulletin, **43**(2), 166–169

Salokhe V M; Gee-Clough D (1988). Coating of cage wheel lugs to reduce soil adhesion. Journal Agricultural Engineering Research, **41**(3), 201–210

Salokhe V M; Gee-Clough D (1989). Applications of enamel coating in agriculture. Journal of Terramechanics, **26**(3 and 4), 275–286

Salokhe V M; Gee-Clough D; Manzoor S; Singh K K (1990). Improvement of the tractive performance of cage wheel lugs by enamel coating. Journal of Agricultural Engineering Research, **45**(3), 209–224

Salokhe V M; Koki M; Sato K (1993). Why does soil not stick to enamel coating? Journal of Terramechanics, **30**(4), 275–283

Schafer R L; Gill W R; Reaves C A (1977). Lubrication plows vs. sticky soil. Agricultural Engineering, **58**(10), 34–38

Sharma V K; Drew L O; Nelson G L (1977). High frequency vibrational effects on soil-metal friction. Transactions of ASAE, **20**(1), 46–51

Shen Z (1982). Mechanism of soil adhesion and its applications. In: Proceedings of the First Conference of Chinese Society for Terrain–Machine Systems, pp 121–123, Wuxi, China

Suminitrado D; Koike M; Konoba T; Yuzawa S; Kuroishi I (1988). A mathematical model to predict the trajectory of soil motion on a moldboard plow surface. In: Proceedings of the Second Asia-Pacific Conference of ISTVS, pp 195–204. Bangkok, Thailand

Sun S; Ren L; Tong J; Chen P (1992). A shovel bucket with steel-cloth pocket by bionics. In: New Technology and Application of Terrain-Vehicles and Machinery, Proceedings of the Third Asia-Pacific Conference of ISTVS, 10–13 August, pp 231–235, Changchun, China

Sun S; Ren L; Tong J (1996a). Design and applications of flexible lining for anti-adhesion. Transactions of the Chinese Society of Agricultural Engineering, **12**(1), 65–70

Sun S; Ren L; Wang Y; Chen D (1996b). Design of anti-adhesion flexible lining steel rings. Journal of Jilin University of Technology, **26**(4), 20–24

Sun J; Sun B; Wei J; Yang R; Ren L; Wu L; Cong Q; Chen B (1991). Measurement and determination of earthworm skin potential related to moving. Journal of Jilin University of Technology, **21**(4), 18–22

Tong J; Lu X; Chen Y; Ren L; Chen B (1990b). Soil adhesion and abrasive wear of PTFE-matrix composites. Transactions of the Chinese Society of Agricultural Engineering, **6**(4), 13–19

Tong J; Ren L; Chen B; Wu L (1990a). Investigation into surface morphology of soil in adhesion interface. Transactions of the Chinese Society of Agricultural Engineering, **6**(3), 1–6

Tong J; Ren L; Chen B (1990c). Reducing adhesion of soil by phosphorus white iron on the basis of bionics principles. In: Proceedings of the 10th International Conference of ISTVS, 20–24 August, pp 57–63, Kobe, Japan

Tong J; Ren L; Sun S; Chen B (1993). Scanning electron microscopy of soil micromorphology at the rubber/soil adhesion. Journal of Chinese Electron Microscopy Society, **12**(5), 348–351

Tong J; Ren L; Chen B; Yan B (1994a). Fractal dimensions of soil particle-size distributions and their effects on soil adhesion behavior. Transactions of the Chinese Society of Agricultural Engineering, **10**(3), 27–33

Tong J; Ren L; Chen Y; Qaisrani A R; Chen B (1994b). Abrasive properties and mechanism of polytetrafluoroethylene and ultra high molecular weight polyethylene. Tribology, **14**(1), 65–72

Tong J; Ren L; Chen B; Qaisrani A R (1994c). Characteristics of adhesion between soil and solid surfaces. Journal of Terramechanics, **32**(2), 93–105

Tong J; Ren L; Chen B (1994d). Geometrical morphology, chemical constitution and wettability of body surfaces of soil animals. International Agricultural Engineering Journal, **3**(1 and 2), 59–68

Tong J; Ren L; Chen B (1995). Chemical constitution and abrasive wear behavior of pangolin scales. Journal of Materials Science Letters, **14**(20), 1468–1470

Tong J; Ren L; Yan J; Ma Y; Chen B (1999). Adhesion and abrasion of several materials against soil. International Agricultural Engineering Journal, **8**(1), 1–22

Tong J; Zhang M; Jiang M; Ren L (1998). Free-abrasive wear of an enamel coating. Journal of Materials Science Letters, **17**(6), 523–525

Tyler S W; Wheatcraft S W (1992). Fractal scaling of soil particle-size distributions: analysis and limitations. Soil Science Society of America Journal, **56**(2), 362–369

Vermeulen G D; Klooster J J; Sprong M C; Verwijs B R (1997). Effect of straight and spiral sugar beet extraction paths and lift acceleration on soil tare and relative soil adherence. Netherlands Journal of Agricultural Science, **45**(1), 163–169

Wang X L; Ichikawa M; Tajiri I; Noro A (1993). Study on prevention of soil adhesion to rotary cover by vibration (Part I). Journal of the Japanese Society of Agricultural Machinery, **55**(4), 41–46

Wang X L; Ito N; Kito K (1996). Study on reducing soil adhesion to machines by vibration. In: Proceedings of the 12th International Conference of ISTVS, 7–10 October, 1996 (Yu Q; Qiu L, eds), pp 539–545. China Machine Press, Beijing, China

Wang Y; Ren L; Li J; Sun S; Zhou R (1997). A model test study on flexible bionics technology of anti-adhesion to dump truck. Transactions of the Chinese Society of Agricultural Engineering, **13**(2), 139–143

Wu S (1982). Polymer Interface and Adhesion. Marcel Dekker, Inc., New York

Xin J (1986). Introduction to Soil Animals. Science Press, Beijing

Xu X; Ren L; Chen B; Cui X; Wang Y; Zhang B; Ge L; Jin G (1990). Preliminary study of chemical composition of body surfaces of typical soil animals. Transactions of the Chinese Society of Agricultural Machinery, **21**(3), 79–83

Yamashiro T (1989). Measurement of piezoelectric constants of a crab shell. Japanese Journal of Applied Physics, **28**(11), 2327–2328

Yamashiro T (1995). Piezoelectric effect of plant leaf. Ferroeletrics, **171**(1–4), 211–124

Yan B; Ren L; Tong J (1996). Effects of soil particle size distribution on friction of soil–solid surfaces. In: Proceedings of the 12th International Conference of ISTVS, 7–10 October (Yu Q; Qiu L, eds), pp 498–505. China Machine Press, Beijing, China

Yin Y; Ren L; Cheng Y; Chen B (1990). A study on cleaning buildup soil in loader shovel on the principle of bionics. Transactions of the Chinese Society of Agricultural Engineering, **6**(4), 1–6

Zhang Y; Han G (1992). Measurement and analysis of work resistance on the magnetic coverer. Journal of Shenyang Agricultural University, **23**(Suppl), 25–28

Zhang J; Sang Z; Gao L (1986). Adhesion and friction between soils and solids. Transactions of the Chinese Society of Agricultural Machinery, **17**(1), 32–40

Zhu H; Tan L; Wu S (1992). An experimental study on the 'comet-type passage-holes' plough of reducing resistance. Transactions of the Chinese Society of Agricultural Machinery, **23**(4), 20–24

Zhuang J; Yi Y; Wu L; Liu X (1992). Effect of magnetic energy on soil electrochemical properties. Journal of Shenyang Agricultural University, **23**(Special Issue), 27–31